AD-A065 108 PENNSYLVANIA STATE UNIV UNIVERSITY PARK DEPT OF CHEMISTRY F/G 7/2
MIXED-METAL CLUSTERS.(U)
FEB 79 W L GLADFELTER, G L GEOFFROY N00014-77-C-0417
UNCLASSIFIED TR-79-1 NL

1 OF 2
AD
A065108

(12)

LEVEL II

Office of Naval Research

Contract N00014-77-C-0417

Task No. NR053-645

Technical Report No. 79-1

"Mixed-Metal Clusters"

by

Wayne L. Gladfelter and Gregory L. Geoffroy

Prepared for Publication

in

Volume 18, Advances in Organometallic Chemistry

Department of Chemistry
The Pennsylvania State University
University Park, Pennsylvania 16802

February 5, 1979

Unclassified

SECURITY CLASSIFICATION OF THIS PAGE (When Data Entered)

REPORT DOCUMENTATION PAGE

READ INSTRUCTIONS BEFORE COMPLETING FORM

1. REPORT NUMBER: Technical Report 79-1
2. GOVT ACCESSION NO.
3. RECIPIENT'S CATALOG NUMBER
4. TITLE (and Subtitle): Mixed-Metal Clusters.
5. TYPE OF REPORT & PERIOD COVERED: Interim Technical Report.
6. PERFORMING ORG. REPORT NUMBER
7. AUTHOR(s): Wayne L. Gladfelter [redacted] Gregory L. Geoffroy
8. CONTRACT OR GRANT NUMBER(s): N00014-77-C-0417
9. PERFORMING ORGANIZATION NAME AND ADDRESS:
Department of Chemistry
The Pennsylvania State University
University Park, Pennsylvania 16802
10. PROGRAM ELEMENT, PROJECT, TASK AREA & WORK UNIT NUMBERS: NR 053-645
11. CONTROLLING OFFICE NAME AND ADDRESS
12. REPORT DATE: 5 Feb [redacted] 1979
13. NUMBER OF PAGES: 93
14. MONITORING AGENCY NAME & ADDRESS (if different from Controlling Office): TR-79-1 / 12 Dec.
15. SECURITY CLASS. (of this report): Unclassified
15a. DECLASSIFICATION/DOWNGRADING SCHEDULE

ACCESSION for
NTIS White Section X
DDC Buff Section
UNANNOUNCED
JUSTIFICATION
BY
DISTRIBUTION/AVAILABILITY CODES
Dist. AVAIL. and/or SPECIAL
A

16. DISTRIBUTION STATEMENT (of this Report)

Distribution unlimited; approved for public release

17. DISTRIBUTION STATEMENT (of the abstract entered in Block 20, if different from Report)

18. SUPPLEMENTARY NOTES

Prepared for publication in Volume 18 of Advances in Organometallic Chemistry

19. KEY WORDS (Continue on reverse side if necessary and identify by block number)

Clusters

Mixed-Metal Clusters

Review

20. ABSTRACT (Continue on reverse side if necessary and identify by block number)

This article is a comprehensive review of the synthesis, properties, reactivity and dynamics of mixed-metal clusters.

DD FORM 1 JAN 73 1473 EDITION OF 1 NOV 65 IS OBSOLETE
S/N 0102-LF-014-6601

Unclassified

SECURITY CLASSIFICATION OF THIS PAGE (When Data Entered)

400 343

LB

Mixed-Metal Clusters

Wayne L. Gladfelter

Department of Chemistry
University of Minnesota
Minneapolis, MN 55455

Gregory L. Geoffroy

Department of Chemistry
The Pennsylvania State University
University Park, PA 16802

I. Introduction

Transition metal cluster compounds are currently under intense scrutiny because of their potential catalytic applications, both as models for understanding catalytic metal surfaces (123-125,127), and as catalysts in their own right (129,141,145). Numerous reviews (7,36,40, 41,90,100,125,127,159) on various aspects of the chemistry and properties of clusters have appeared including recent reviews of tetranuclear carbonyl clusters (40), high nuclearity metal carbonyl clusters (41), hydrido transition-metal clusters (90), structural and bonding patterns in cluster chemistry (159), clusters and surfaces (125), very small metallic and bimetallic clusters and their relevance to the cluster-surface analogy (127), and NMR studies of clusters (7). The purpose of this particular review is to address an increasingly important subset of clusters, those which contain a mixture of different transition metals in their metal framework.

Mixed-metal clusters are of interest from three principle perspectives. First, they should prove valuable as precursors for the preparation of bimetallic and multimetallic <u>heterogeneous</u> catalysts (17,141,145). Such catalysts could be prepared by allowing clusters to absorb onto catalyst supports such as SiO_2 and Al_2O_3, followed by pyrolysis to remove the ligands. This technique could yield multimetallic catalysts with precisely defined compositions and high dispersion, if the degree of aggregation which occurs during the pyrolysis step is minimal. Secondly, mixed-metal clusters may find important applications in <u>homogeneous</u> catalysis. In particular, because of the different reactivities of the different metals present in mixed-metal clusters, multi-metal homogeneous catalysts may show reactivity patterns significantly different than those of homometallic

clusters. Finally, the low-symmetry of mixed-metal clusters makes them useful for probing various aspects of the reactivity and molecular dynamics of clusters. For example, the dynamic properties of $H_2FeRu_2Os(CO)_{13}$ were clearly resolved because of its mixed-metal character (77). The consequent low symmetry allowed the carbonyls to become nonequivalent and distinguishable by ^{13}C NMR spectroscopy. Likewise, the specific sites of substitution in $H_2FeRu_3(CO)_{12}(PMe_2Ph)$ were determined by NMR spectroscopy because of the inherent low symmetries of the isomers of this complex (82).

In this review, we have attempted to compile a comprehensive listing of all the mixed-metal clusters which have been prepared. It has been necessary to adhere to a specific definition of a mixed-metal cluster and the following two criteria have been set by us for detailed coverage in this review:

1. Only transition metals are considered under the mixed-metal category.
2. By definition, a cluster must contain at least three metals and a portion of the cluster must contain a closed polyhedron.

These criteria have arbitarily ruled out many compounds which may be of interest to the reader. We mention several of these in a non-comprehensive section at the end of this review.

The clusters which we have surveyed are tabulated in Table 1. Clusters within this table are listed under the earliest transition metal which they contain within their framework. The groups of the periodic table are listed in succession and within each group the metals are arranged by period. The entries within each metal listing are further categorized according to the size of the clusters, with smaller clusters listed before

larger ones. For illustration, $FeCo_2(CO)_8(C_2Ph_2)$ appears before $FeNi_2(Cp)_2(CO)_5$, but both are listed prior to $FeCo_3H(CO)_{12}$.

Some interesting statistics are revealed in Table 1. Of the 161 entries, clusters with four metals dominate having 83 separate entries. Three-metal clusters are next with 56. There are 11 five-metal clusters, 10 six-metal clusters, but only 1 cluster with more than six metals. The largest mixed-metal cluster is $[Fe_6Pd_6H_5(CO)_{24}]^{3-}$ with 12 metals (111). Forty percent of the mixed-metal clusters shown in Table 1 contain iron (64 entries). The next largest contributor is cobalt with 53 entries. The ranking by element with respect to number of entries is as follows: Fe (64) > Co (53) > Os (45) > Ru (32) > Pt (26) > Ni (19) > Rh (16), Re (16) > Mo (12), W (10) > Mn (8) > Ir (7) > Cr (4), Cu (4), Au (4) > Pd (3) > Ta (2) > Ti (1), Zr (1), V (1), Tc (1).

II. Synthesis

It has often been said that noticeably few metal clusters have been prepared by designed or rational synthetic procedures (52,55). Indeed, most clusters have been prepared by placing together a variety of reagents, allowing them to react, and then examining the reaction mixtures to see what compounds have been prepared. This is particularly true of mixed-metal clusters, and a real need exists for the development of synthetic procedures which can be used for the designed synthesis of particular compounds.

Examination of the methods that have been used to prepare the mixed-metal clusters listed in Table 1 reveals that the majority have been synthesized via four general types of reactions: 1) pyrolysis, 2) addition to coordinatively-unsaturated compounds, 3) redox condensations,

and 4) reaction of carbonylmetalates with metal halides. Each of these reaction types is discussed below and several examples are given in each case. These are followed by sections on miscellaneous synthetic reactions and possible synthetic strategies for future mixed-metal cluster syntheses.

A. Pyrolysis Reactions

Pyrolysis reactions generally involve heating two or more stable compounds of different metals together, presumably to give fragments which then combine to yield the mixed-metal clusters. The amount of heat necessary to drive these reactions varies considerably, but in many cases simply stirring the reactants at ambient temperature is sufficient. These reactions are not generally adaptable to designed synthesis. They usually yield a variety of products which must be separated by chromatography to give moderate to very low yields of the mixed-metal clusters.

1. Pyrolysis of Two Monomeric Species. Relatively few clusters have been prepared by the pyrolysis of two monomeric compounds and only two examples are given. Stone and coworkers (28,30) allowed $H_2Os(CO)_4$ to react with several Pt(0) complexes, and, although most of the reactions involved an unsaturated starting complex and will accordingly be discussed in Section IIB, $Os_2Pt(CO)_7(PPh_2Me)_3$ resulted from the reaction shown in eq. 1.

$$H_2Os(CO)_4 + Pt(PPh_2Me)_4 \xrightarrow[3\ days]{25^\circ} Os_2Pt(CO)_7(PPh_2Me)_3 \quad (1.3\%) \quad (1)$$

McCarley and coworkers (117) recently prepared Ta_4Mo_2 and Ta_5Mo clusters by the pyrolysis of $TaCl_5$ with $MoCl_5$ according to the stoichiometries shown in eqs. 2 and 3.

$$5\ TaCl_5 + MoCl_5 + 5\ Al \xrightarrow[\substack{60\%\ AlCl_3\\40\%\ NaCl}]{320°C,\ 3\ days} Ta_5MoCl_{15} + 5\ AlCl_3 \qquad (2)$$

$$12\ TaCl_5 + 6\ MoCl_5 + 14\ Al \xrightarrow[\substack{50\%\ AlCl_3\\50\%\ NaCl}]{320°C,\ 3\ days} 3\ Ta_4Mo_2Cl_{16} + 14\ AlCl_3 \qquad (3)$$

Work-up afforded salts of the anions $[(Ta_4Mo_2Cl_{12})Cl_6]^{2-}$ and $[(Ta_5MoCl_{12})Cl_6]^{2-,3-}$ and these were fully characterized. Although niobium and tantalum had been previously reported (135) to form mixed-metal cluster compounds of the type $Ta_{6-x}Nb_xBr_{14}$, discrete species were not isolated and McCarley's work thus represents the first successful characterization of mixed-metal halide clusters.

2. Pyrolysis of Metal-Carbonyl Dimers. Metal-carbonyl dimers have proven to be useful reagents for the synthesis of mixed-metal clusters. This is particularly true for Fe and Co clusters, since $Fe_2(CO)_9$ and $Co_2(CO)_8$ are readily available starting materials. The prediction of the reaction products is usually fruitless. However, examination of the available data indicates that the initial dimeric unit is preserved in approximately half the reactions. Typical examples are illustrated in eqs. 4-10.

$$Fe_2(CO)_9 + Co(Cp)(CO)_2 \xrightarrow[\text{light petroleum}]{65°C,\ 15\ min} \underset{\text{(moderate yield)}}{Fe_2Co(Cp)(CO)_9} \qquad (4)^{(102)}$$

$$Fe_2(CO)_9 + Rh(Cp)(CO)_2 \xrightarrow[\text{light petroleum}]{\Delta,\ 20\ min} \underset{\text{(low yield)}}{Fe_2Rh(Cp)(CO)_9} \qquad (5)^{(102)}$$

$$Fe_2(CO)_9 + Rh(Cp)(CO)_2 \xrightarrow[\text{light petroleum}]{\Delta,\ 5\ h} \begin{array}{l} FeRh_2(Cp)_2(CO)_6 \text{ (trace) +} \\ Fe_3Rh(Cp)(CO)_{11} \text{ (trace) +} \\ \underset{\text{(very low yield)}}{Fe_2Rh_2(Cp)_2(CO)_8} \end{array} \qquad (6)^{(102)}$$

$$Fe_2(CO)_9 + Pt(L)_4 \xrightarrow[\text{benzene}]{25°C,\ 17\ h} Fe_2Pt(CO)_8L_2 \text{ (low yield)} \qquad (7)^{(28)}$$

$$Fe_2(CO)_9 + H_2Os(CO)_4 \xrightarrow[\text{heptane}]{25°C,\ 3\ h} Fe_2Os(CO)_{12}\ (70\%) + H_2FeOs_3(CO)_{13}\ (6\%) \qquad (8)^{(121)}$$

$$Fe_2(CO)_9 + H_2Os_2(CO)_8 \xrightarrow[\text{heptane}]{25°C} FeOs_2(CO)_{12}\ (20\%) \qquad (9)^{(121)}$$

$$Co_2(CO)_8 + H_2Os(CO)_4 \xrightarrow[\text{heptane}]{25°C,\ 5\ h} CoOs_2(CO)_{11}\ (20\%) + H_2Co_2Os_2(CO)_{12}\ (10\%) \qquad (10)^{(121)}$$

The first mixed-metal cluster $HFeCo_3(CO)_{12}$ was synthesized by Chini and coworkers in 1959 using a reaction of this type (35).

$$Fe(CO)_5 + Co_2(CO)_8 \xrightarrow[\text{acetone}]{\Delta,\ 10\ h} HFeCo_3(CO)_{12}\ (90\%) \qquad (11)$$

This particular reaction may proceed via the initial disproportionation of $Co_2(CO)_8$ to give $[Co(CO)_4]^-$ which then undergoes redox condensation with $Fe(CO)_5$.

The preferred preparative method for $FeCo_2(CO)_9S$, I, is condensation of the dimers $Fe_2(CO)_6S_2$ and $Co_2(CO)_8$, eq. 12 (99).

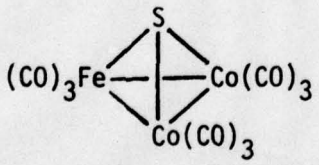

I

$$Fe_2(CO)_6S_2 + Co_2(CO)_8 \xrightarrow{\text{hexane}} FeCo_2(CO)_9S\ (56\%) \qquad (12)$$

Interestingly, this cluster was initially discovered by careful analysis of the products from a hydroformylation reaction of thiophene using

$Co_2(CO)_8$ as the catalyst in a steel bomb (99). The sulfur was apparently abstracted from thiophene and the iron apparently came from the reaction vessel.

3. Pyrolysis of Metal Carbonyl Clusters. The pyrolysis of clusters in the presence of monomers, dimers, or other clusters usually requires much more severe reaction conditions than the previously descussed examples. Common starting materials such as $Ru_3(CO)_{12}$ and $Os_3(CO)_{12}$ are themselves quite stable compounds. The reaction of $Ru_3(CO)_{12}$ with a variety of compounds has yielded many mixed-metal clusters as illustrated by eqs. 13-18.

$$Ru_3(CO)_{12} + Fe(CO)_5 \xrightarrow{110°C,\ 24\ h} Fe_2Ru(CO)_{12} + FeRu_2(CO)_{12} + H_2FeRu_3(CO)_{13} \quad (13)^{(101,161)}$$

$$Ru_3(CO)_{12} + Os_3(CO)_{12} \xrightarrow[xylene]{175°C,\ 90\ h,\ CO} Ru_2Os(CO)_{12} + RuOs_2(CO)_{12} \quad (14)^{(96)}$$

$$Ru_3(CO)_{12} + Pt(dppe)_2 \xrightarrow[benzene]{25°C,\ 6\ days} Ru_2Pt(CO)_8(dppe)_5\ (21\%) \quad (15)^{(30)}$$

$$Ru_3(CO)_{12} + Pt(PMe_2Ph)_4 \xrightarrow[benzene]{25°C,\ 7\ days} Ru_2Pt(CO)_7(PMe_2Ph)_2 \quad (16)^{(28)}$$

$$Ru_3(CO)_{12} + Pt(PPh_3)_4 \xrightarrow[benzene]{25°C,\ 7\ days} RuPt_2(CO)_5(PPh_3)_3\ (20\%) \quad (17)^{(28,30)}$$

$$Ru_3(CO)_{12} + Pt[PPh(OMe)_2]_4 \xrightarrow[benzene]{25°C,\ 5\ days} RuPt_2(CO)_4[PPh(OMe)_2]_4\ (27\%) \quad (18)^{(30)}$$

The higher temperature and longer reaction time for eq. 14 compared to eq. 13 reflects the greater difficulty of breaking $Os_3(CO)_{12}$ into fragments.

The reactions of various platinum derivatives with $Ru_3(CO)_{12}$, eqs. 15-18, were explored by Stone and coworkers (28,30). As seen by comparison of

eqs. 14-17, the exact product which resulted was very dependent on the particular platinum complex employed. All of the reactions involved phosphine transfer from platinum to ruthenium during the course of the reaction. X-ray structural analysis of $RuPt_2(CO)_5(PPh_2Me)_3$, II, shows that this cluster has the ruthenium-bound phosphine located in an axial position unlike the other substituted triangular clusters which possess the substituted ligand in an equatorial position (120).

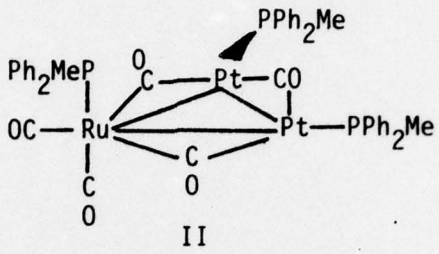

II

B. Addition of Coordinatively-Unsaturated Species

This synthetic method has only recently become important. It is closely related to the pyrolysis technique since coordinatively-unsaturated species are presumably formed during pyrolysis by dissociation of ligands or cleavage of metal-metal bonds. These coordinatively-unsaturated species apparently are the key intermediates which condense to give the cluster products. The addition of a metal nucleophile to a preformed coordinatively-unsaturated compound, in general, occurs under much milder conditions, and these reactions appear quite adaptable to design. They also normally give much higher yields of the cluster products than do the pyrolysis reactions.

$H_2Os_3(CO)_{10}$, whose structure is shown in III, has been extensively used by Stone and coworkers (67,68) to synthesize mixed-metal clusters which contain the Os_3 framework. Several of these reactions, including Johnson et al.'s adaptation with $Co_4(CO)_{12}$ (23), are summarized in Scheme I.

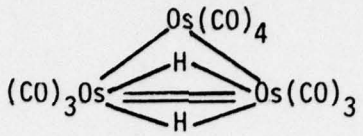

III

Scheme I

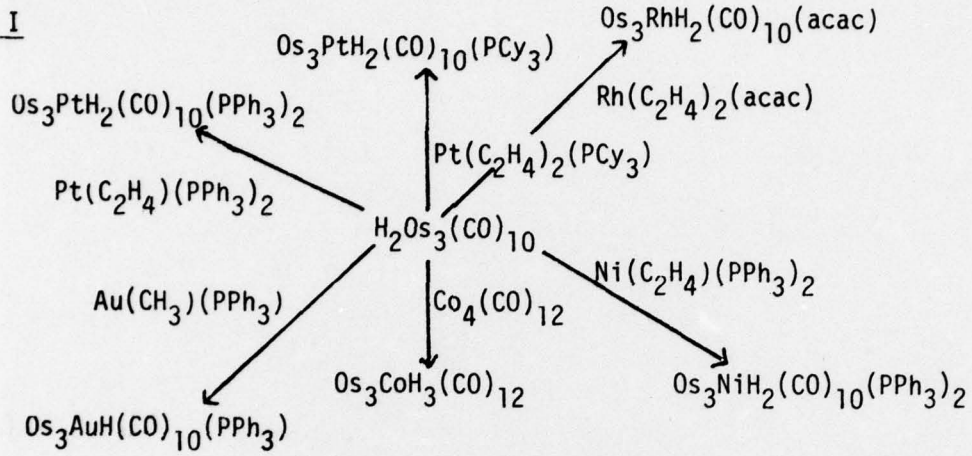

X-ray structural analyses have demonstrated that $Os_3PtH_2(CO)_{10}(PCy_3)$ (67) and $Os_3CoH_3(CO)_{12}$ (23) have tetrahedral structures. The other species shown in Scheme I likely have similar structures.

Stone and coworkers (68) have also employed the unsaturated dimer $H_2Re_2(CO)_8$, IV (22),

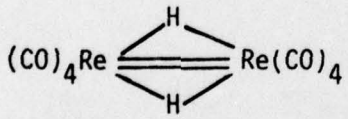

IV

to prepare the clusters $Re_2PtH_2(CO)_9(PPh_3)$ and $Re_2AuH(CO)_9(PPh_3)$, eqs. 19 and 20.

$$H_2Re_2(CO)_8 + Pt(C_2H_4)_2(PPh_3) \rightarrow Re_2PtH_2(CO)_9(PPh_3) \qquad (19)$$

$$H_2Re_2(CO)_8 + Au(CH_3)(PPh_3) \rightarrow Re_2AuH(CO)_9(PPh_3) \qquad (20)$$

The reaction of nucleophilic Pt(0), Pd(0), and Ni(0) complexes with unsaturated metal-metal bonds has been extended by Stone and coworkers (18,19) to include carbene and carbyne derivatives, eqs. 21 and 22.

$$W[C(OMe)Ph](CO)_5 + Pt(C_2H_4)_2\{PMe(t\text{-}Bu)_2\} \xrightarrow[\text{toluene}]{-20°C}$$

$$WPt_2\{\mu\text{-}C(OMe)Ph\}(CO)_6\{PMe(t\text{-}Bu)_2\}_2 \qquad (21)^{(18)}$$

V (50%)

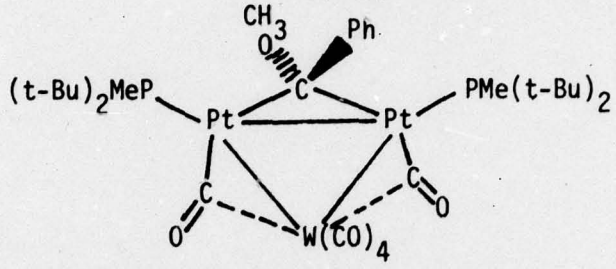

V

$$W(C\text{-}C_6H_4Me)(Cp)(CO)_2 + Pt(C_2H_4)_3 \rightarrow W_2Pt(C\text{-}C_6H_4Me)_2(Cp)_2(CO)_4 \qquad (22)^{(19)}$$

Note that the carbene ligand migrated from W to a position bridging the Pt-Pt bond during the course of reaction 21. On the basis of these various synthetic studies, Stone (19) has proposed a formal analogy between the addition of metal nucleophiles to olefins, metal carbenes, and doubly bonded metal-metal compounds and a similar analogy between the addition of metal nucleophiles to alkynes, metal carbynes, and triply bonded metal-metal compounds, Scheme II.

Scheme II

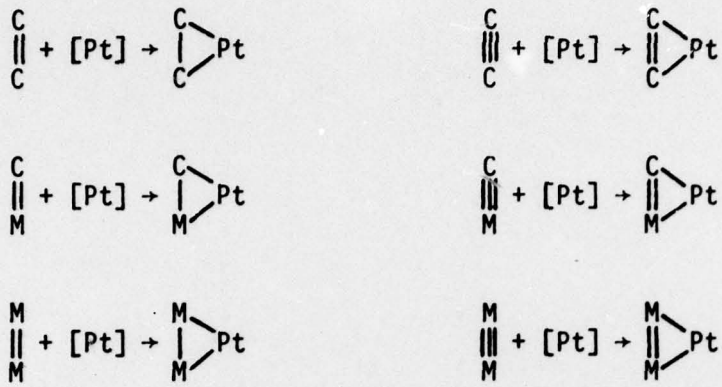

Mixed-metal clusters have also been prepared by the reaction of coordinatively-unsaturated monomeric Pt(0) complexes with $H_2Os(CO)_4$, eqs. 23 and 24.

$$H_2Os(CO)_4 + Pt(C_2H_4)(PPh_3)_2 \xrightarrow[\text{benzene}]{25°C,\ 22\ h} \underset{(11\%)}{OsPt_2(CO)_5(PPh_3)_3} \qquad (23)^{(28)}$$

$$H_2Os(CO)_4 + Pt(C_2H_4)_2L \rightarrow Os_2Pt_2H_2(CO)_8L_2 \qquad (24)^{(67)}$$

Shapley and coworkers (144) have studied the addition of metal hydride complexes to "lightly stabilized" metal clusters such as $Os_3(CO)_{10}(NCCH_3)_2$ and $Os_3(CO)_{10}(COT)_2$. The acetonitrile and cyclooctene ligands are readily displaced to give an unsaturated species which then appears to oxidatively add the metal hydride. Me_3NO has also been used to oxidize and remove one of the carbonyls of $Os_3(CO)_{12}$ to generate a similar coordinately unsaturated species. Due to the relatively mild conditions which are used in these reactions, the initial products do not further react and hence give an interesting series of open clusters in high yields, eqs. 25 and 26.

$$Os_3(CO)_{12} + Me_3NO{\cdot}2H_2O \xrightarrow[CH_3CN]{} "Os_3(CO)_{11}(CH_3CN)" \xrightarrow[\text{benzene}]{HRe(CO)_5}$$

$$ReOs_3H(CO)_{16} \quad (50\%) \qquad (25)$$

$$Os_3(CO)_{10}(NCCH_3)_2 + \text{excess } HRe(CO)_5 \xrightarrow{\text{benzene}} Re_2Os_3H_2(CO)_{20} \qquad (26)$$

VI (90%)

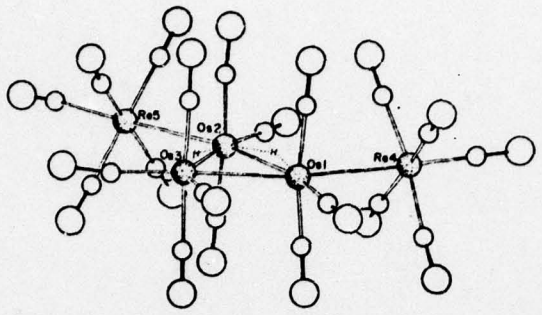

VI

Similar reactions employing $WH(Cp)(CO)_3$ yielded closed tetranuclear clusters, eq. 27 (48).

$$Os_3(CO)_{10}(NCCH_3)_2 + \text{excess } WH(Cp)(CO)_3 \xrightarrow[\text{toluene}]{\Delta,\ 0.5\ h} WOs_3H(Cp)(CO)_{12} \ (30\%)$$

$$+ WOs_3H_3(Cp)(CO)_{11} \ (10\%) \qquad (27)$$

C. Redox Condensations

The reaction of a carbonylmetalate with a neutral metal carbonyl has been labelled a "redox condensation" by Chini (40,41) and has been as widely used as pyrolysis reactions for synthesizing mixed-metal clusters. Carbonylmetalates usually react rapidly with most neutral carbonyls even under very mild conditions. A large number of mixed-metal hydride clusters have been formed via this type of reaction, primarily because the initial products are anionic clusters which in many cases may be protonated to yield the neutral hydride derivative.

The reaction of carbonylmetalates with monomeric and dimeric carbonyls has yielded many mixed-metal clusters, as illustrated by the reactions shown in eqs. 28-31.

$$[Mn(CO)_5]^- + Fe(CO)_5 \xrightarrow{\text{diglyme}} [MnFe_2(CO)_{12}]^- \quad (28)^{(15)}$$

$$[Mn(CO)_5]^- + Ni_2(Cp)_2(CO)_2 \xrightarrow[\text{THF}]{\Delta,\ 0.5\ h} [MnNi_2(Cp)_2(CO)_5]^- \ (65\%) \quad (29)^{(87)}$$

$$[MoCp(CO)_3]^- + Fe_2(CO)_9 \xrightarrow[\text{THF}]{25°C,\ 0.5\ h} [Mo_2Fe_2(Cp)_2(CO)_{10}]^{2-} \quad (30)^{(88)}$$
(65%)

$$[WCp(CO)_3]^- + Fe_2(CO)_9 \xrightarrow[\text{THF}]{25°C,\ 0.5\ h} [W_2Fe_2(Cp)_2(CO)_{10}]^{2-} \quad (31)^{(88)}$$
(69%)

A series of trigonal bipyramidal clusters of the general formula $[M_2Ni_3(CO)_{16}]^{2-}$ (M = Cr, Mo, W) were prepared by Dahl and coworkers (134) via the reaction shown in eq. 32.

$$[M_2(CO)_{10}]^{2-} + Ni(CO)_4 \xrightarrow[\text{THF}]{\Delta,\ 1.5\ h} [M_2Ni_3(CO)_{16}]^{2-} \quad (30\text{-}70\%) \quad (32)$$
(M = Cr, Mo, W)

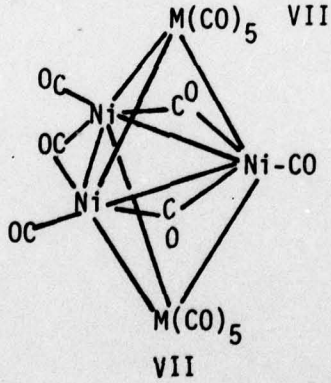

VII

The reaction of carbonylmetalates with trinuclear clusters provides in many cases a convenient synthesis of tetranuclear clusters. This reaction was first explored by Knight and Mays (105,106) who allowed $[Mn(CO)_5]^-$ and $[Re(CO)_5]^-$ to react with trimeric clusters of the iron

triad. A summary of the products which they obtained using $Os_3(CO)_{12}$ as the starting trimer is shown in Scheme III.

Scheme III

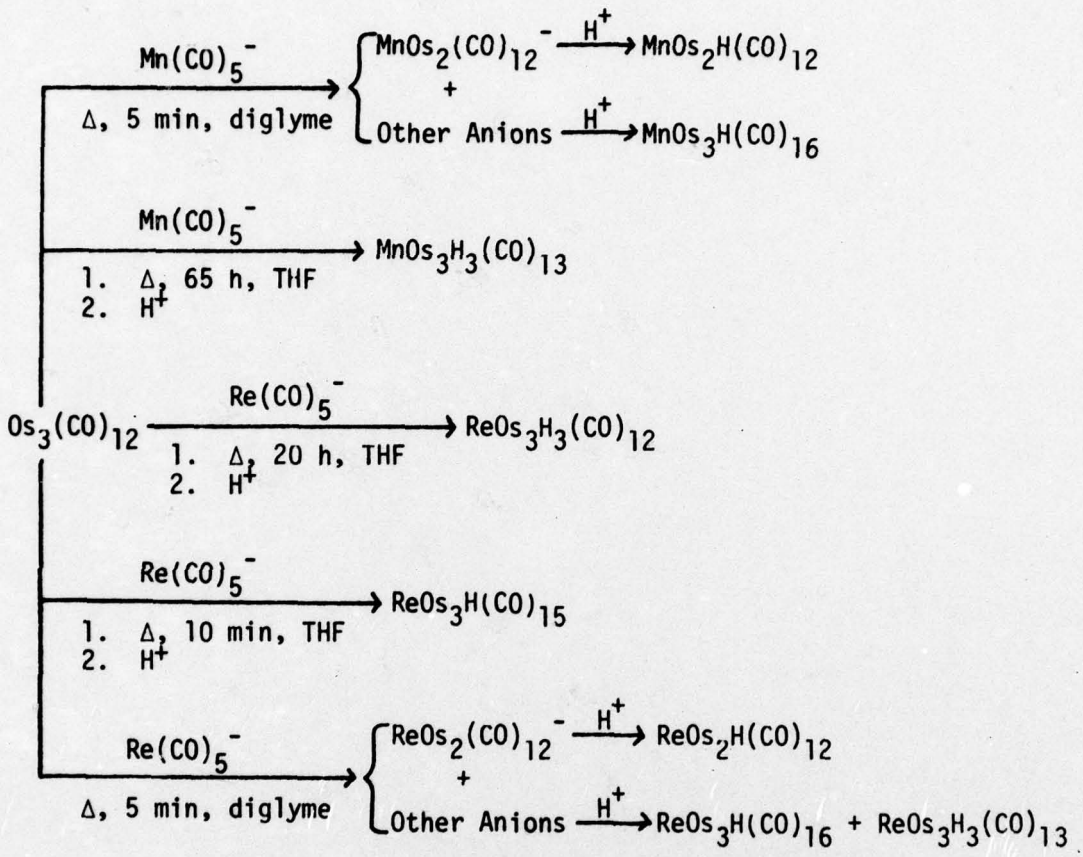

Of particular mechanistic interest are the tetranuclear clusters which were formed. As indicated in Scheme III, the carbon monoxide/metal ratio in the tetranuclear products decreased as the rigor of the reaction conditions increased. It is reasonable to assume that this also corresponds to an increase in the number of metal-metal bonds. It was suggested that the clusters $ReOs_3H(CO)_{16}$ and $ReOs_3H(CO)_{15}$ are intermediates along the reaction path to the final tetrahedral cluster $ReOs_3H_3(CO)_{13}$. Unfortunately, only the crystal structure of $ReOs_3H(CO)_{15}$,

VIII, has been reported (47), but $ReOs_3H(CO)_{16}$ and $ReOs_3H(CO)_{13}$ were proposed to have structures IX and X, respectively (106).

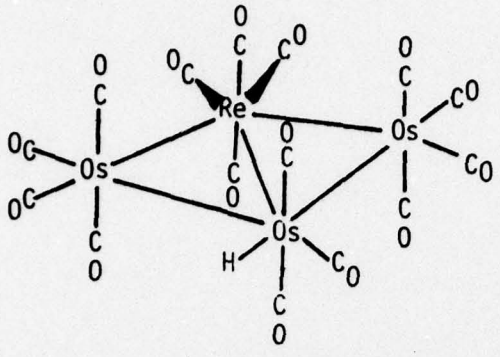

VIII

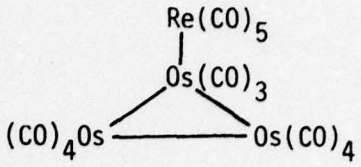

IX

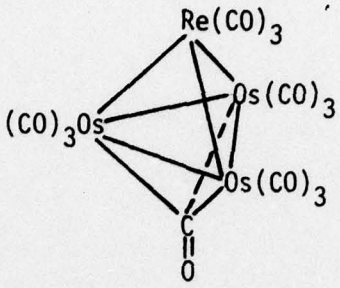

X

The reaction of $[Fe(CO)_4]^{2-}$ and $[Co(CO)_4]^-$ with metal carbonyl trimers has also been shown to be useful for the preparation of mixed-metal clusters, eqs. 33 and 34 (78, 147).

$$Ru_3(CO)_{12} + [Fe(CO)_4]^{2-} \xrightarrow[THF]{\Delta,\ 2h} \xrightarrow{H^+} H_2FeRu_3(CO)_{13} \quad (50\%) \qquad (33)^{(78)}$$

$$Ru_3(CO)_{12} + [Co(CO)_4]^- \xrightarrow[THF]{\Delta,\ 3h} \xrightarrow{H^+} HCoRu_3(CO)_{13} \quad (60\%) \qquad (34)^{(147)}$$

The 50% yield of $H_2FeRu_3(CO)_{13}$ from eq. 33 represents a significant improvement over previous pyrolysis methods (101,161). These particular reactions can be scaled up to produce several grams of the clusters in a single reaction, and consequently these mixed-metal clusters are readily available for reactivity studies. Clusters which contain three different metals within the cluster framework were prepared by similar reactions, eqs. 35-37.

$$\left.\begin{matrix} Ru_2Os(CO)_{12} \\ + \\ RuOs_2(CO)_{12} \end{matrix}\right\} + [Fe(CO)_4]^{2-} \xrightarrow[THF]{\Delta,\ 2h} \xrightarrow{H^+} \begin{matrix} H_2FeRu_2Os(CO)_{13}\ (36\%) + \\ H_2FeRuOs_2(CO)_{13}\ (74\%) \end{matrix} \quad (35)^{(78)}$$

$$\left.\begin{matrix} Ru_2Os(CO)_{12} \\ + \\ RuOs_2(CO)_{12} \end{matrix}\right\} + [Co(CO)_4]^{2-} \xrightarrow[THF]{\Delta,\ 3h} \xrightarrow{H^+} \begin{matrix} HCoRu_2Os(CO)_{13}\ (35\%) + \\ HCoRuOs_2(CO)_{13}\ (25\%) \end{matrix} \quad (36)^{(147)}$$

$$Fe_2Ru(CO)_{12} + [Co(CO)_4]^- \xrightarrow[THF]{\Delta,\ 2\ h} [CoFe_2Ru(CO)_{13}]^- \quad (37)^{(147)}$$

$$FeRu_2(CO)_{12} + [Co(CO)_4]^- \xrightarrow[THF]{\Delta,\ 1.25\ h} [CoFeRu_2(CO)_{13}]^- \quad (38)^{(147)}$$

D. Reaction of Carbonylmetalates with Metal Halides

Carbonylmetalates will displace a halide from a metal halide complex to yield a metal-metal bonded species, eq. 39. With di- and polyhalide

$$[M(CO)_x]^{n-} + Cl\text{-}ML_n \rightarrow Cl^- + (CO)_xM\text{-}ML_n \quad (39)$$

complexes or with dimeric carbonylmetalates, cluster compounds can result. The configuration of the metal-metal bonded product is very dependent upon the nature of the starting complex. For example, reaction of trans-$PtCl_2(pyridine)_2$ with $[Co(CO)_4]^-$ gives a linear Co-Pt-Co species, eq. 40 (25,128), whereas a Co_2Pt cluster results from the reaction of

$$\underline{trans}\text{ - }PtCl_2(pyridine)_2 + [Co(CO)_4]^- \rightarrow (CO)_4Co\text{-}\underset{\displaystyle NC_5H_5}{\overset{\displaystyle NC_5H_5}{Pt}}\text{-}Co(CO)_4 \quad (40)$$

$PtCl_2(dppe)$ with $[Co(CO)_4]^-$, eq. 41 (59).

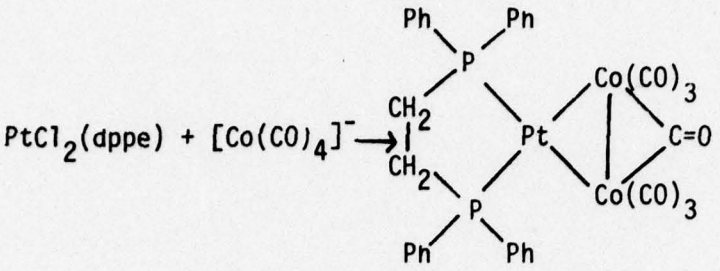

(41)

However, reaction of cis-$PtCl_2(PEt_3)_2$ with $[Co(CO)_4]^-$ leads to the formation of the tetra- and pentanuclear products shown in eq. 42 (20).

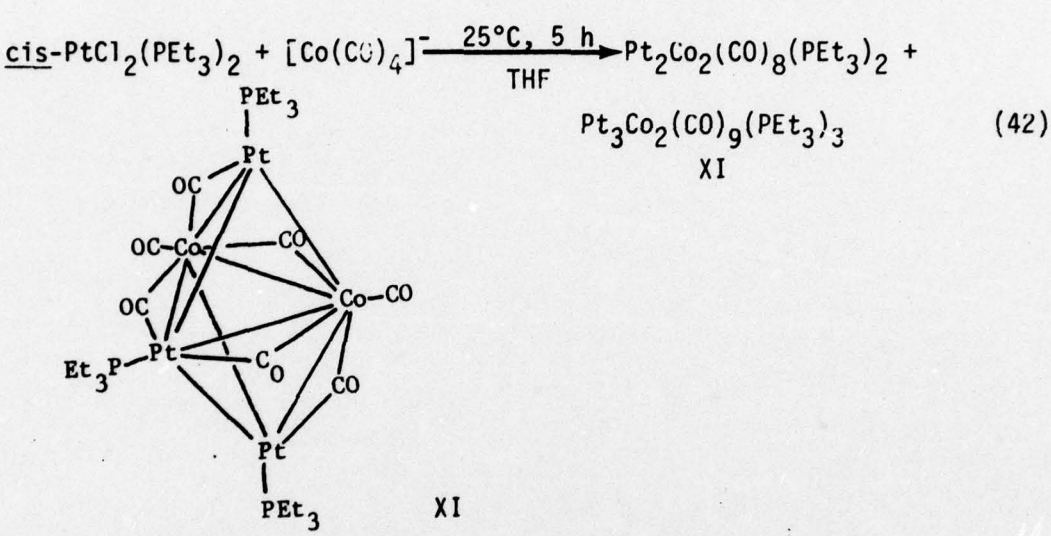

(42)

XI

Further examples of this synthetic technique are shown in eqs. 43-46.

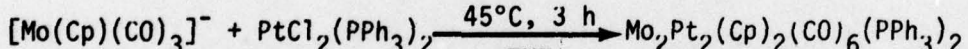

(43)[26]

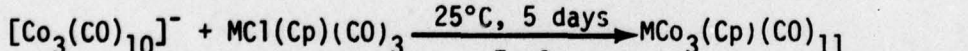

(44)[137]

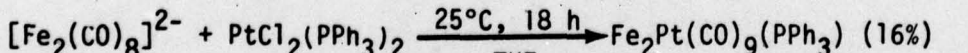

(45)[43]

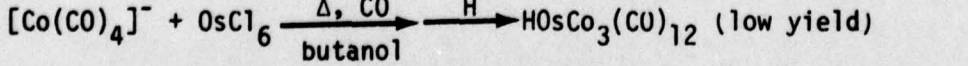

(46)[103]

The last reaction illustrates the use of a pure metal halide complex as a reagent in syntheses of this type.

E. Other Methods

Many metal clusters have been prepared by reactions which do not fall into any of the above catagories. Space does not permit a discussion of all of these, but we will illustrate a few with examples. Somewhat surprisingly, photochemical techniques have only been used to produce two mixed-metal clusters and these were prepared by Sheline and coworkers (66,109) by photolysis of mixtures of $M_2(CO)_{10}$ (M = Tc, Re) and $Fe(CO)_5$, eqs. 47 and 48.

$$Re_2(CO)_{10} + Fe(CO)_5 \xrightarrow[Et_2O]{h\nu} [ReFe_2(CO)_{12}]^- \quad (47)^{(66)}$$

$$Tc_2(CO)_{10} + Fe(CO)_5 \xrightarrow[THF]{h\nu} [TcFe_2(CO)_{12}]^- \quad (48)^{(109)}$$

The yield of the anionic clusters was reduced when the photochemical reactions were conducted in hydrocarbon solutions, and in these cases linear triatomic $M_2Fe(CO)_{14}$ species were isolated.

Chini has synthesized a series of mixed-metal clusters which contain various combinations of the metals within the cobalt triad (113). The reactions shown in eqs. 49-53 are illustrative.

$$RhCl_3 \cdot 3H_2O + [Co(CO)_4]^- \xrightarrow[H_2O]{5\ h} Co_3Rh(CO)_{12}\ (70\text{-}80\%) \quad (49)$$

$$Co_2(CO)_8 + [RhCl(CO)_2]_2 \xrightarrow[hexane]{3\ days} Co_2Rh_2(CO)_{12}\ (80\text{-}90\%) \quad (50)$$

$$[Co(CO)_4]^- + [IrI(CO)_5]^- \xrightarrow[H_2O]{25°C} Co_2Ir_2(CO)_{12}\ (70\text{-}80\%) \quad (51)$$

$$[Rh(CO)_4]^- + [IrI(CO)_5]^- \xrightarrow[H_2O,\ quickly]{CO} Rh_3Ir(CO)_{12}\ (10\%) \qquad (52)$$

$$[Ir(CO)_4]^- + [RhCl_2(CO)_2]^- \xrightarrow[H_2O]{CO} Rh_2Ir_2(CO)_{12}\ (60\%) \qquad (53)$$

Although these reactions could be classified as the addition of a carbonylmetalate to a metal halide complex, they do not appear to represent simple addition and instead are relatively complex.

Chini and coworkers (75) have also prepared $[Rh_5Pt(CO)_{15}]^-$, XII, by the scrambling of the two anionic clusters shown in eq. 54.

$$[Pt_{12}(CO)_{24}]^{2-} + 5[Rh_{12}(CO)_{13}]^{2-} \xrightarrow[THF]{25°C,\ CO,\ 1\ atm} 12[Rh_5Pt(CO)_{15}]^- \qquad (54)$$
XII

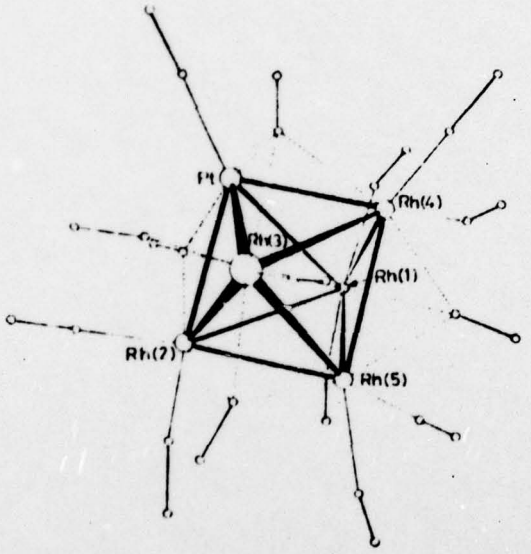

XII

It is surprising that only one product resulted from this reaction, but $[Rh_5Pt(CO)_{15}]^-$ must be particularly stable since it also forms from the metal halide salts, eq. 55 (75).

$$5RhCl_3 \cdot 3H_2O + [PtCl_6]^{2-} + 20H^- + 25CO \xrightarrow[MeOH]{25°C,\ 1\ atm} [Rh_5Pt(CO)_{15}]^- + 10CO_2 + 21Cl^- + 10H_2O \qquad (55)$$

NMR studies have shown that $[Rh_5Pt(CO)_{15}]^-$ maintains its integrity in solution but it does react with carbon monoxide to form $[Rh_4Pt(CO)_{14}]^{2-}$ (34,75).

Bruce and coworkers (2,3) have prepared several mixed-metal clusters which contain copper. Unlike most of the compounds discussed in this review, these particular mixed-metal clusters possess acetylides as ligands rather than carbon monoxide. $Ir_2Cu_4(PPh_3)_2(C_2Ph)_8$, XIII, results from the reaction shown in eq. 56.

$$IrCl(CO)(PPh_3)_2 + [Cu(C_2Ph)]_n \xrightarrow[\text{benzene}]{\Delta,\ 36\ h} Ir_2Cu_4(PPh_3)_2(C_2Ph)_8\ (61\%) \quad (56)$$

(Next Page)

XIII[3,45]

Also isolated from the above reaction was a small amount (4%) of a complex which analyzed for $IrCu_3(PPh_3)_3(C_2Ph)_2$ but whose structure has not yet been reported. The analogous $Rh_2Cu_4(PPh_3)_2(C_2Ph)_8$ cluster was prepared by a similar procedure. $Ir_2Cu_4(PPh_3)_2(C_2Ph)_8$ reacts with $Fe_2(CO)_9$ to yield purple crystals of $Fe_2Ir_2Cu_4(PPh_3)_2(C_2Ph)_8$ (2). Spectral evidence indicates that the Ir_2Cu_4 core is unchanged in the product and the iron atoms are simply π-bound to the acetylide ligands. A somewhat similar reaction was used to prepare $Fe_2Ru(Cp)(CO)_6(PPh_3)(C_2Ph)$, except in this case the iron atoms are part of the triangular framework of the cluster, eq. 57 (1,27).

$$Ru(Cp)(PPh_3)_2(C\equiv CPh)\cdot CuCl + Fe_2(CO)_9 \xrightarrow[\text{benzene}]{25°C,\ 18\ h} Fe_2Ru(Cp)(CO)_6(PPh_3)(C_2Ph) \quad (57)$$

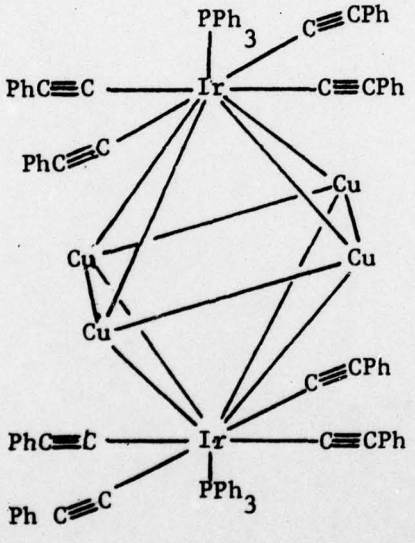
PPh3
CCPh
PhCC
Ir
CCPh
PhCC
Cu
Cu
Cu
Cu
CCPh
PhCC
Ir
CCPh
Ph CC
PPh3

XIII

F. Synthetic Strategies

Although serendipity still plays an important role in the successful synthesis of a desired cluster, sufficient precedented reactions now exist to allow one to derive an initial synthetic strategy. This is especially true for triangular and tetranuclear clusters and may even extend to larger clusters. In this section we have summarized several reactions that may be adaptable to design.

It appears that the most logical way to synthesize any desired triangular or tetranuclear cluster is to begin with monomeric complexes and build the desired cluster by adding one metal at a time. As outlined in Scheme 4, we suggest that to prepare a desired tetrahedral cluster one would start by allowing two monomeric organometallic complexes to react to yield a metal-metal dimer. This in turn could react with another monomeric complex to produce a triangular cluster which could then be capped by the addition of a fourth monomeric complex.

Scheme 4

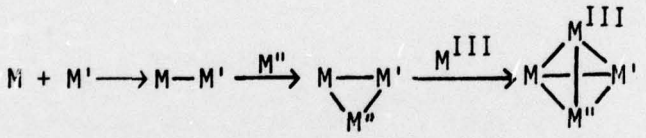

The first step in this synthetic approach is to form a metal-metal dimer. Numerous organometallic dimers have been prepared, and tabulated below are examples of the reaction types which appear most useful.

Reaction of a Metal Halide Complex with a Carbonylmetalate

$$[MnCO)_5]^- + ReCl(CO)_5 \rightarrow MnRe(CO)_{10} \qquad (58)^{(160)}$$

Reaction of a Neutral Carbonyl with a Carbonylmetalate

$$[Mn(CO)_5]^- + Cr(CO)_6 \xrightarrow[\text{diglyme}]{160\text{-}170^\circ} [CrMn(CO)_{10}]^- + CO \qquad (59)^{(16)}$$

Coupling of Metal Hydride and Metal Alkyl Complexes

$$Zr(Cp)_2(CH_3)_2 + MoH(Cp)(CO)_3 \rightarrow (Cp)_2(CH_3)Zr\text{-}Mo(Cp)(CO)_3 + CH_4 \qquad (60)^{(131)}$$

Bridge Assisted Reactions

$$Fe(CO)_4(AsMe_2Cl) + [Mn(CO)_5]^- \rightarrow (CO)_4Fe\text{-}AsMe_2\text{-}Mn(CO)_5 \xrightarrow{h\nu} \qquad (61)^{(61)}$$

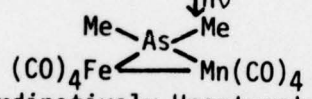

Addition of Metal Hydrides to Coordinatively-Unsaturated Complexes

$$H_2Os(CO)_4 \xrightarrow[-CO]{\Delta} "H_2Os(CO)_3" \xrightarrow{H_2Os(CO)_4} Os_2H_2(CO)_8 + H_2 \qquad (62)^{(122)}$$

Much less effort has been directed toward the rational preparation of triangular clusters as has been given to the synthesis of dimers. A survey of the methods used to prepare existing triangular clusters suggests that the reaction types listed below hold the most promise for the designed synthesis of new triangular species.

Addition of a Dimeric Carbonylmetalate to a Neutral Carbonyl

$$Na_2[Fe_2(CO)_8] + Fe(CO)_5 \rightarrow Na_2[Fe_3(CO)_{11}] + 2CO \qquad (63)^{(43)}$$

Addition of a Dimeric Carbonylmetalate to a Metal Halide Complex

$$Na_2[Fe_2(CO)_8] + \underline{cis}\text{-}PtCl_2(PPh_3)_2 \xrightarrow[THF]{25°C,\ 18\ h} Fe_2Pt(CO)_8(PPh_3)_2 + 2NaCl \quad (64)^{(43)}$$

Addition of a Monomeric Carbonylmetalate to a Neutral Dimer

$$[Ni(Cp)(CO)]_2 + [Mn(CO)_5]^- \rightarrow [MnNi_2(Cp)_2(CO)_5]^- \quad (65)^{(87)}$$

Condensation of Monomeric and Dimeric Neutral Carbonyl Complexes

$$Co(Cp)(CO)_2 + Fe_2(CO)_9 \rightarrow Fe_2Co(Cp)(CO)_9 \quad (66)^{(102)}$$

$$H_2Os(CO)_4 + Co_2(CO)_8 \rightarrow OsCo_2(CO)_{11} \quad (67)^{(121)}$$

Addition Across Multiple Metal-Metal Bonds

$$H_2Re_2(CO)_8 + Pt(C_2H_4)_2(PPh_3) \rightarrow Re_2PtH_2(CO)_9(PPh_3) \quad (68)^{(94)}$$

$$(Cp)_2Mo_2(CO)_4 + Pt(PPh_3)_4 \rightarrow Mo_2Pt(Cp)_2(CO)_4(PPh_3)_2 \quad (69)^{(57)}$$

Addition of a Carbonylmetalate to a Dihalide Dimer

$$(Cp)(CO)_2\underset{I}{Mo}\text{-}\underset{I}{Mo}(Cp)(CO)_2 + [Fe(CO)_4]^{2-} \rightarrow Mo_2Fe(Cp)_2(CO)_8 + 2I^- \quad (70)^{(57)}$$

The two types of reactions which appear most useful for the preparation of tetranuclear clusters are those given below.

Addition of a Carbonylmetalate to a Neutral Carbonyl Trimer

$$[Fe(CO)_4]^{2-} + Ru_2Os(CO)_{12} \xrightarrow{\Delta} \xrightarrow{H^+} H_2FeRuOs_2(CO)_{13} \quad (71)^{(78)}$$

Addition of a Metal Hydride to an Unsaturated Trimer

$$Os_3(CO)_{10}(NCCH_3)_2 + WH(Cp)(CO)_3 \rightarrow WOs_3H(Cp)(CO)_{12} \quad (72)^{(27)}$$

In principle, both of these types of reactions could be employed to build up large clusters by the addition of a carbonylmetalate or a metal hydride across the triangular faces of tetranuclear clusters. These reactions, however, have yet to be demonstrated.

III. Methods of Characterization

The spectroscopic methods that one chooses to characterize a particular compound will depend on the character of that compound as well as the type of information that one wishes to gain. For example, neutral clusters are readily characterized by mass spectrometry, whereas this method has been of little use for characterizing anionic clusters. Likewise, if one is interested in the location of a hydride ligand or the site of phosphine or phosphite substitution, the most versatile tools are NMR spectroscopy and x-ray diffraction. We cannot, because of space limitation, discuss all the common characterization techniques in detail but instead we only highlight a few of the more important features.

A. Mass Spectrometry

Mass spectrometry has been an extremely useful characterization tool for neutral organometallic clusters except for those few cases which have extremely high molecular weights or possess ligands such as PPh_3 which reduce the volatility of the compound. Mass spectrometry has not been a useful characterization technique for ionic clusters because these compounds are simply not volatile enough to study using conventional

electron-impact techniques. However, there is some hope that with the development of field desorption techniques ionic clusters as well as neutrals will be able to be analyzed by mass spectrometry (146).

A typical mass spectrum is that of $H_2FeRu_2Os(CO)_{13}$ shown in Figure 1. In general, the spectrum of a mixed-metal cluster will show the parent ion, as well as ions corresponding to loss of each of the carbonyl and the hydrogen ligands all the way down to the bare metal core. Three features of the mass spectrum are important for characterizing a compound. First, the position of the parent ion gives an indication of the molecular weight of the compound. One has to be cautious, however, and insure that the ion which is observed is indeed the parent. Most clusters will show the parent ion in their mass spectrum, but its intensity is variable.

Secondly, the carbonyl loss pattern can indicate the number of carbonyl ligands that a cluster possesses. One can easily determine the number of carbonyls simply by counting the ions that are separated by 28 mass units due to successive loss of each of the carbonyls. For example, in the spectrum of $H_2FeRu_2Os(CO)_{13}$, Figure 1, ions corresponding to loss of all 13 carbonyls are observed.

Finally, the isotopic distribution of the parent ion can serve as a fingerprint for a given metal composition. The isotopic distribution of the parent ion of $H_2FeRuOs_2(CO)_{13}$ is shown in Figure 2. The wide isotopic distribution from m/e 911 to m/e 895 arises because iron, ruthenium and osmium have 4, 9, and 7 naturally occurring isotopes of appreciable abundances. The various combinations taken together with the appropriate weighting factors gives the calculated distribution shown in Figure 2. If one is unsure of the metal composition of a particular

cluster, one can compare the experimental isotopic distribution with that calculated for a number of trial compositions and can often uniquely determine the correct composition.

Mixtures of compounds are often difficult to analyze using electron-impact mass spectrometry because of overlapping mass peaks from fragment ions of all the compounds present. However, chemical ionization mass spectrometry has proven useful for analysis of such mixtures since only the parent ions of each compound present is normally observed. If metal carbonyls are studied and the instrument is operated in the negative ion mode, only ions corresponding to the parent minus one carbonyl are seen. For example, the mixture of compounds $Ru_3(CO)_{12}$, $Ru_2Os(CO)_{12}$, $RuOs_2(CO)_{12}$, and $Os_3(CO)_{12}$ has proven extremely difficult to separate using normal chromatographic or fractional crystallization techniques. We found that the electron impact mass spectrum of this mixture of compounds showed essentially a continuum of mass peaks beginning with the parent ion of $Os_3(CO)_{12}$ at m/e 906 (78). However, the chemical ionization mass spectrum of this mixture showed ions at m/e 878, 789, 700, and 611 corresponding to the parent ions minus one carbonyl for each of the four clusters. From the relative intensities of the peaks, we were able to estimate the relative ratios of the four trimers in the mixture as 1:2:2:1 (78).

B. Infrared Spectroscopy

Infrared spectroscopy is most useful for identifying a known compound via comparison to published infrared data. In general, it is not possible to determine the structure or composition of a cluster by its infrared spectrum alone, although the spectrum can provide several useful indicators. The region which has proven most useful is from 1700-2200 cm^{-1} where

carbonyl ligands generally absorb. The remainder of the infrared spectrum has so far been useful only for determining the presence or absence of other types of ligands. For example, a cluster which contains PPh_3 will show the characteristic ligand vibrations below 1600 cm^{-1}. In the carbonyl region, carbonyls which are bound to a single metal atom normally appear between 2200-1900 cm^{-1} whereas carbonyls which bridge 2 or 3 metals are generally in the 1900-1700 cm^{-1} region. Triply-bridging carbonyls generally lie lowest. One should use caution in assigning a carbonyl in the 1850-1950 cm^{-1} region to a terminal or bridging position since the charge of the cluster can substantially effect the position of the bands in the infrared spectrum. Anionic clusters, for example, generally show all their carbonyl vibrations at lower energy than the corresponding vibrations of a neutral cluster of similar composition.

For illustration, Figure 3 shows the infrared spectra of $H_2FeRu_3(CO)_{13}$, $H_2FeRu_2Os(CO)_{13}$, $H_2FeRuOs_2(CO)_{13}$, and $H_2FeOs_3(CO)_{13}$ (78). Only the structure of $H_2FeRu_3(CO)_{13}$ has been determined by x-ray diffraction (79) but the remarkable similarity of the infrared spectra shown in Figure 3 indicates that the other three clusters must have similar structures. In each case the compounds show a set of bands between 2100 and 1950 cm^{-1} which may be attributed to the 11 terminal carbonyls and a grouping of bands near 1850 cm^{-1} which were assigned to the bridging carbonyls.

C. Electronic Absorption Spectroscopy

Electronic absorption spectroscopy is generally not very useful for characterizing mixed-metal clusters, although most mixed-metal clusters are highly colored and show rich UV-visible spectra. The bands which are observed may be attributed in most cases to transitions between orbitals involved in the metal-metal bonding. A comparison of the

electronic absorption spectra of $H_2FeRu_3(CO)_{13}$, $H_2FeRu_2Os(CO)_{12}$, and $H_2FeRuOs_2(CO)_{13}$ is shown in Figure 4 (78). The spectra are virtually identical, showing only a spectral blue shift as the osmium content increases. This spectral shift is consistent with the notion that the observed bands are due to metal-metal transitions which increase in energy as the strength of the metal-metal bonds increases as more third row metal character is incorporated. Similar shifts have been observed in the spectra of $Fe_3(CO)_{12}$, $Fe_2Ru(CO)_{12}$, $FeRu_2(CO)_{12}$, $Ru_3(CO)_{12}$ and $Os_3(CO)_{12}$ (35,156,161), and detailed electronic absorption spectral studies of these latter compounds have conclusively shown that the electronic transitions are between orbitals involved in the metal-metal bonding (156).

D. Nuclear Magnetic Resonance Spectroscopy

Nuclear magnetic resonance spectroscopy has proven to be quite useful for characterizing metal clusters and particularly clusters which have hydride ligands (7,90,95). Like infrared spectroscopy, one cannot determine a complete structure of an unknown cluster by measurement of its NMR spectrum, but some insight into structural features may be obtained. ^1H NMR has been most useful for detecting the presence of hydride ligands and in many cases has led to an accurate assessment of their chemical environment. Although the hydride resonances for clusters generally lie in the chemical shift range τ 15-45, for structurally similar clusters, the chemical shifts of hydride ligands seldom differ by more than a few ppm. Thus by comparing the chemical shift of an unknown compound with those reported for related compounds, one can usually narrow the possibilities for the hydride's chemical environment. ^1H NMR spectroscopy is extremely useful for determining if the several hydrides

that are present in a polyhydride cluster are in equivalent or non-equivalent positions. However, as discussed in Section V, metal clusters are normally fluxional at room temperature and one must be careful to insure that the static spectrum has been obtained when one is trying to infer structural information.

^{13}C NMR spectroscopy has largely been used to study the fluxional properties of metal clusters, but structural information has been obtained in selected cases. It has been amply demonstrated that resonances due to bridging carbonyls lie much further downfield than those of terminally bound carbonyls in the same cluster. Furthermore, the terminal carbonyls in mixed-metal clusters such as $H_2FeRu_2Os(CO)_{13}$ often group together in regions characteristic of carbonyls bound to a given metal (77). For example, in $H_2FeRu_2Os(CO)_{13}$ the resonances of the carbonyls bound to osmium occur in the 168-177 ppm region, the resonances of those bound to ruthenium occur in the 184-189 ppm region, and the resonances of those terminally bound to iron occur in the 204-211 ppm region, Figure 6 (77).

E. Mossbauer Spectroscopy

Mossbauer spectroscopy has thus far only been used to characterize mixed-metal clusters which contain iron, but it has been useful in deducing structures in several instances. The principal utility of the technique

has been in determining whether or not the several iron atoms that are in a cluster are in equivalent environments. An application to the characterization of mixed-metal clusters comes from the compounds $Fe_2Co(Cp)(CO)_9$ and $Fe_2Rh(Cp)(CO)_9$. Two different environments for the iron atoms were observed for the cobalt compound, whereas only a simple doublet was seen in the spectrum of the rhodium derivative indicating that both iron atoms are in equivalent positions (102). Structures XIX and XX were suggested on the basis of this data.

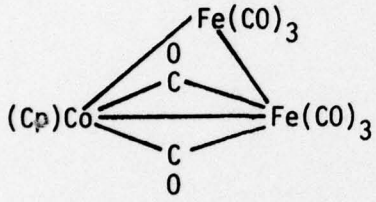

XIX

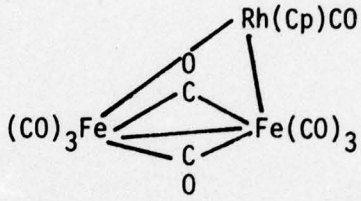

XX

Likewise, doublets with broadened lines were observed in the spectra of $Fe_2Rh_2(Cp)_2(CO)_8$ and $Fe_3Rh(Cp)(CO)_{11}$, indicating nonequivalent iron atoms as was subsequently confirmed by x-ray analysis (102,50,51).

Mossbauer spectroscopy can indeed be a very useful technique for characterizing iron-containing clusters, but it will continue to be of limited use for other metals.

F. Structure Determination by X-ray and Neutron Diffraction

The best way to determine the structure of any compound is to determine its structure by x-ray or neutron diffraction. Indeed, as indicated in Table I, many mixed-metal clusters have had their structures examined by x-ray crystallography and at least one by

neutron diffraction. Space does not allow presentation of the structures of all these clusters, and the reader is refered to the original articles.

G. Chromatographic Properties

Although liquid chromatography has been extensively used to separate mixed-metal clusters, very little attention has been given to using this technique to identify compounds. With the advent of analytical high pressure liquid chromatography instruments, one has the capability to identify previously prepared compounds by comparison of retention times, much as gas chromatography has been used in studies of organic compounds. A typical chromatogram that may be obtained for a mixture of clusters with a commercial high-performance analytical instrument is shown in Figure 5 and illustrates the kind of separation that can now be achieved. Workers within a group with their own analytical instrument could accumulate a list of retention times of known compounds under a standard set of chromatographic conditions, and then simply compare retention times for compounds resulting from new reactions. One must be cautious, however, since it is not unlikely for several compounds to have similar retention times, and this technique can at best only complement other identification methods. In our hands, we have found analytical high-pressure liquid chromatography extremely useful for following the course of reactions and for suggesting the identity of products (62). Microporous silica columns such as Waters Associates' μ-Porasil column appear most useful.

IV. Reactivity

There have been relatively few studies of the reactivity of mixed-metal clusters, in part because few have been available in sufficient quantity to study. The majority of investigations have centered on

ligand substitution reactions employing Group V donor ligands. These are discussed first followed by brief discussions of the acid-base chemistry of mixed-metal clusters and their reactions with H_2, CO, and alkynes. Finally, we present those few studies in which mixed-metal clusters have been employed as catalysts.

A. Ligand Substitution Reactions

Substitution of the neutral cluster $FeCo_3H(CO)_{12}$ with phosphorous donor ligands has been extensively studied by several groups (54,89,153). Cooke and Mays (54) noted that mono-, di-, and trisubstituted derivatives could be prepared, depending on the initial reaction conditions and reagent ratios, eq. 73.

$$FeCo_3H(CO)_{12} + L \rightarrow FeCo_3H(CO)_{12-n}L_n \qquad (n = 1\text{-}3) \qquad (73)$$

$L = PPh_3$, PPh_2Me, PEt_3, $P(OPh)_3$, $P(OPr)_3$

Infrared and ^{57}Fe Mossbauer spectral studies indicated that substitution in these derivatives occurs exclusively at cobalt with one ligand per cobalt atom in the trisubstituted derivatives (54). Only with the chelating dppe ligand was a tetrasubstituted product formed, eq. 74.

$$FeCo_3H(CO)_{12} + 2\ dppe \rightarrow FeCo_3H(CO)_{10}(dppe) + FeCo_3H(CO)_8(dppe)_2 \qquad (74)$$

The ^{57}Fe Mossbauer spectrum of $FeCo_3H(CO)_8(dppe)_2$ indicated the presence of a 1:3 ratio of two isomers. The less abundant isomer was attributed to a cluster with both dppe ligands attached to cobalt atoms, while the second isomer was assigned a structure with one dppe ligand bridging to the iron. It was noted that $FeCo_3H(CO)_{12}$ was considerably more inert to substitution than the isoelectronic $Co_4(CO)_{12}$.

Kaesz and coworkers (89) recently reported the reaction of $FeCo_3H(CO)_{12}$ with $P(OMe)_3$, and they were able to isolate a tetrasubstituted product in which the fourth $P(OMe)_3$ ligand was bound to iron. The structure of $FeCo_3H(CO)_9\{P(OMe)_3\}_3$ was determined by x-ray diffraction at -139°C and is shown in XXI. The hydride ligand was located on the C_3 axis situated below the Co_3 face.

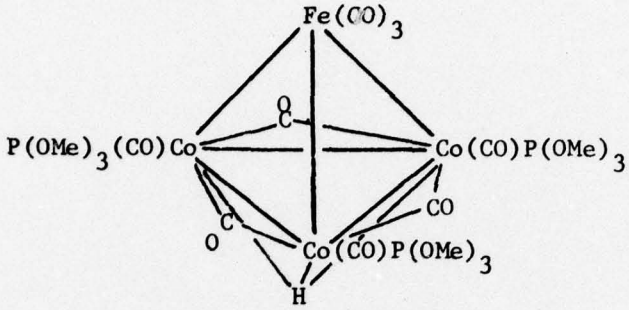

XXI

An independent neutron diffraction study by Bau and coworkers (153) on the same cluster confirmed the hydrogen's position. These results were particularly significant since the location of the hydride ligand in the parent $FeCo_3H(CO)_{12}$ cluster had generated considerable discussion since its initial report. Unfortunately, the quadrupole moment of the cobalt nuclei had prevented observation of a ^1H NMR signal for the hydride ligand in $FeCo_3H(CO)_{12}$ and any of its derivatives (54,89).

Cooke and Mays (53) also studied the substitution of the anionic clusters $[FeCo_3(CO)_{12}]^-$ and $[MnFe_2(CO)_{12}]^-$, eqs. 75 and 76.

$$[FeCo_3(CO)_{12}]^- + L \xrightarrow[\text{acetone}]{\Delta,\ 12\ h} [FeCo_3(CO)_{11}L]^- \qquad (75)$$

$L = PPh_3,\ PMePh_2,\ P(OPr)_3$

$$[MnFe_2(CO)_{12}]^- + L \xrightarrow[\text{acetone}]{\Delta,\ 2.5\ h} [MnFe_2(CO)_{11}L]^- \qquad (76)$$

$L = PPh_3,\ PMePh_2.\ P(OPr)_3$

Unlike $FeCo_3H(CO)_{12}$, only monosubstituted derivatives could be isolated with $[FeCo_3(CO)_{12}]^-$. This was attributed to a greater stabilization of the anionic cluster by the π-accepting CO's (53).

Reaction of $FeCo_2(CO)_9S$ with a series of phosphines (31,133) and isocyanides (126) has yielded mono-, di-, and trisubstituted derivatives, eqs. 77 and 78. ^{57}Fe Mossbauer spectra of the phosphine substituted

$$FeCo_2(CO)_9S + L \rightarrow FeCo_2(CO)_{9-n}SL_n \qquad (n = 1\text{-}3) \qquad (77)$$

$L = PPh_3,\ P(n\text{-}Bu)_3$

$$FeCo_2(CO)_9S + CN\text{-}\underline{t}\text{-}Bu \rightarrow FeCo_2(CO)_{9-n}S(CN\text{-}\underline{t}\text{-}Bu)_n \qquad (n = 2,\ 3) \qquad (78)$$

derivatives indicated that substitution at cobalt occurs prior to substitution at iron (31). Unfortunately, no crystallographic evidence has been obtained for any of these derivatives, and the precise stereochemistry has not been resolved, even with the aid of ^{13}C NMR spectra (9). The problem is compounded with the isocyanide ligands since several isomers of the trisubstituted derivatives are formed.

Rossetti and coworkers (133) have investigated the kinetics and mechanism of the substitution of $FeCo_2(CO)_9S$ and its derivatives. Both associative and dissociative paths were observed in each of the three substitution steps. However, the first and second phosphine ligands substituted predominantly by an associative pathway, although the rate of the first substitution was much faster than the second. It was

suggested that initial attack occurs by the phosphine on the triangular face opposite the sulfur atom. Substitution of the third ligand was slow and occurred principally via a dissociative pathway.

We have recently studied the substitution of $FeRu_3H_2(CO)_{13}$ with a series of phosphorous donor ligands and prepared several mono- and disubstituted derivatives, eq. 79 (82).

$$FeRu_3H_2(CO)_{13} + L \rightarrow FeRu_3H_2(CO)_{12}L + FeRu_3H_2(CO)_{11}L_2 \qquad (79)$$

$L = P(i\text{-}Pr)_3$, PPh_3, $PMePh_2$, PEt_2Ph, $P(OMe)_3$, $P(OEt_2)Ph$, PMe_2Ph, PMe_3

$^{31}P\{^1H\}$ and ^1H NMR data indicate that the monosubstituted derivatives exist in the two isomeric forms XXII and XXIII.

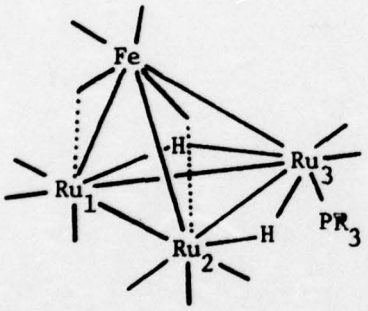

XXII

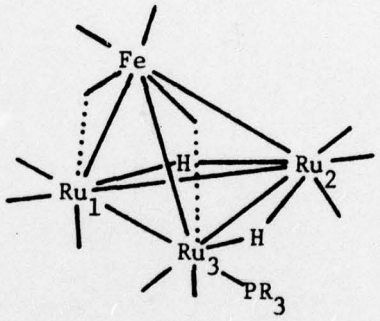

XXIII

These isomers were found to interconvert on the NMR time scale and this process will be discussed in more detail in Section V. The disubstituted derivatives appeared to form at a slower rate than the monosubstituted derivatives, and attempts at further substitution led to break-up of the cluster. When basic phosphines such as PEt_2Ph were employed, deprotonation of the starting cluster occurred to yield $[FeRu_3H(CO)_{13}]^-$. Cooke and Mays (54) observed similar deprotonation in their study of $FeCo_3H(CO)_{12}$.

One would like to be able to predict at which metal of a mixed-metal cluster substitution would occur. From the limited data available, the only reasonable conclusion that can be drawn is that Co substitutes more readily than Fe in mixed Fe-Co clusters. Clearly, further studies are needed to build-up sufficient data to confidently address this question.

$FeCo_2(CO)_9S$ has recently been shown to undergo a unique reaction in which the cluster itself acts as a donor ligand, eq. 80 (132).

$$FeCo_2(CO)_9S + Cr(CO)_5(THF) \rightarrow \underset{\text{XXVI}}{FeCo_2(CO)_9S\text{-}Cr(CO)_5} \qquad (80)$$

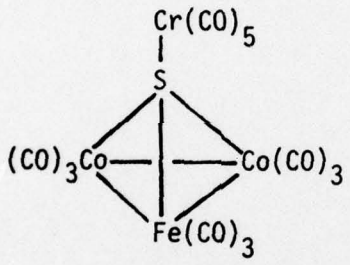

XXIV

X-ray structural data indicate that essentially no changes in the geometry of the $FeCo_2S$ cluster occurs upon complexation to $Cr(CO)_5$.

B. Acid-Base Reactions

In many cases anionic mixed-metal clusters can be protonated to yield neutral hydride clusters and likewise neutral hydride clusters can be deprotonated to yield anionic species. For example, $[CoRu_3(CO)_{13}]^-$ is the initial product resulting from the addition of $[Co(CO)_4]^-$ to $Ru_3(CO)_{12}$. This cluster can be isolated either as its $[(Ph_3P)_2N]^+$ salt or protonated with H_3PO_4 to give $CoRu_3H(CO)_{13}$, eq. 81 (147).

$$[Co(CO)_4]^- + Ru_3(CO)_{12} \xrightarrow[THF]{\Delta,\ 1\ h} [CoRu_3(CO)_{13}]^- \xrightarrow{H^+} CoRu_3H(CO)_{13} \quad (81)$$

$$\downarrow [(Ph_3P)_2N]^+$$

$$[(Ph_3P)_2N][CoRu_3(CO)_{13}]$$

Protonation reactions such as these are usually accomplished using noncomplexing, nonoxidizing acids such as H_3PO_4. One should be careful in protonating anionic clusters since many of the corresponding neutral hydride clusters are thermally unstable and rapidly decompose. For example, attempted protonation of $[FeCo_3(CO)_{10}(C_2Ph_2)]^-$ did not give the expected $FeCo_3H(CO)_{10}(C_2Ph_2)$ but rather $FeCo_2(CO)_8(C_2Ph_2)$, eq. 82 (53).

$$[FeCo_3(CO)_{10}(C_2Ph_2)]^- + H^+ \rightarrow FeCo_2(CO)_8(C_2Ph_2) \quad (82)$$

Likewise, we have prepared the anionic clusters $[CoFeRu_2(CO)_{13}]^-$ and $[CoFe_2Ru(CO)_{13}]^-$, but all attempts to isolate the corresponding neutral hydride clusters after protonation have failed, apparently because of their instability (147).

Deprotonation reactions are not so facile. Bases such as OH^- and NR_3 have to be used with caution since they can lead to cluster degradation via attack of the base on the carbonyl ligands. Shore and coworkers (94) recently reported a deprotonation method using KH, and we (80) have successfully employed this procedure to deprotonate $FeRu_3H_2(CO)_{13}$, eq. 83.

$$FeRu_3H_2(CO)_{13} + KH \xrightarrow[THF]{25°C,\ 24\ h} H_2 + K[FeRu_3H(CO)_{13}] \quad (83)$$

The only study of the kinetics of a protonation reaction was conducted by Cooke and Mays (53) who studied the deuterium isotope effect on the rate of protonation of $[FeCo_3(CO)_{12}]^-$ and $[FeCo_3(CO)_{11}\{P(O\text{-}\underline{i}\text{-}Pr)_3\}]^-$. Large deuterium isotope effects were observed and for $[FeCo_3(CO)_{12}]^-$

k_H/k_D = 17.8 ± 1 whereas for $[FeCo_3(CO)_{11}\{P(O\text{-}i\text{-}Pr)_3\}]^-$, k_H/k_D = 8.3 ± 1. These large values were attributed to "tunneling" of the proton through the ligand barrier to reach its site below the Co_3 face.

C. Reactions with H_2 and CO

A number of metal clusters have been demonstrated to react with H_2, often leading to replacement of one CO by two hydride ligands. Kaesz and coworkers (107) first demonstrated this reaction for a mixed-metal cluster when they prepared $FeRu_3H_4(CO)_{12}$ from $FeRu_3H_2(CO)_{13}$, eq. 84. Other examples are shown in eqs. 85-87.

$$FeRu_3H_2(CO)_{13} + H_2 \xrightarrow[\text{hexane}]{\Delta,\ 6\ h} FeRu_3H_4(CO)_{12} + CO \qquad (84)^{(107)}$$

$$Ru_4H_2(CO)_{13} + H_2 \xrightarrow[\text{hexane}]{\Delta,\ 2\ min} Ru_4H_4(CO)_{12} + CO \qquad (85)^{(107)}$$

$$CoRu_3H(CO)_{13} + H_2 \xrightarrow[\text{hexane}]{\Delta,\ 2\ h} CoRu_3H_3(CO)_{12} + CO \qquad (86)^{(81)}$$

$$WOs_3H(Cp)(CO)_{12} + H_2 \xrightarrow[\text{toluene}]{\Delta,\ 0.5\ h} WOs_3H_3(Cp)(CO)_{11} + CO \qquad (87)^{(48)}$$

This type of reaction appears to have considerable generality and we suspect that many clusters which have one or two hydride ligands can be converted into tri- and tetrahydrides, respectively. Those reactions appear favored because of the loss of steric crowding upon replacing one CO with two hydrogens. We know of no examples in which hydride clusters have been prepared from non-hydride clusters with the same metal framework via a reaction of this type nor of any related reactions which lead to clusters with more than four hydrides. As can be seen by comparing the reaction conditions given in eqs. 84-86, the relative reactivity is greatly dependent upon the specific metals involved, even for isoelectronic clusters.

A number of mixed-metal clusters have been demonstrated to react with CO, often under quite mild conditions, eqs. 88-95.

$$FeRu_3H_4(CO)_{12} + CO \rightarrow FeRu_3H_2(CO)_{13} \quad (88)^{(80)}$$

$$FeRu_3H_2(CO)_{13} + CO \rightarrow Ru_3(CO)_{12} + Fe(CO)_5 + H_2 \quad (89)^{(80)}$$

$$[FeRu_3H(CO)_{13}]^- + CO \rightarrow [Ru_3H(CO)_{11}]^- + Fe(CO)_5 \quad (90)^{(80)}$$

$$FeRu_2OsH_2(CO)_{13} + CO \rightarrow Ru_2Os(CO)_{12} + Fe(CO)_5 + H_2 \quad (91)^{(80)}$$

$$FeRuOs_2H_2(CO)_{13} + CO \rightarrow RuOs_2(CO)_{12} + Fe(CO)_5 + H_2 \quad (92)^{(80)}$$

$$[CoRu_3(CO)_{13}]^- + CO \rightarrow Ru_3(CO)_{12} + [Co(CO)_4]^- \quad (93)^{(80)}$$

$$[Co_4Ni_2(CO)_{14}]^{2-} + CO \rightarrow [NiCo_3(CO)_{11}]^- + Ni(CO)_4 + [Co(CO)_4]^- \quad (94)^{(38)}$$

$$[Rh_5Pt(CO)_{15}]^- + CO \rightarrow [Rh_4Pt(CO)_{14}]^{2-} \quad (95)^{(34,75)}$$

The reaction expressed in eq. 88 is the reverse of the hydrogen addition, eq. 84, and represents one of the few demonstrated cases of reductive-elimination of H_2 from an intact cluster. The tetranuclear clusters which have been studied appear to consistently fragment in the presence of CO to produce a metal carbonyl trimer and a monomeric fragment in highly specific fashions.

D. Reactions with Alkynes

The only examples of the reaction of mixed-metal clusters with alkynes are shown in eqs. 96-98.

$$[FeCo_3(CO)_{12}]^- + PhC{\equiv}CPh \xrightarrow[\text{acetone}]{\Delta,\ 5\ h} [FeCo_3(CO)_{10}(PhC_2Ph)]^- \quad (96)^{(53)}$$

$$FeRu_3H_2(CO)_{13} + RC{\equiv}CR' \xrightarrow[\text{hexane}]{\Delta,\ 15\ min} FeRu_3(CO)_{12}(RC_2R') \quad (97)^{(74)}$$

R, R' = Ph, Me
R = Ph; R' = Me

isomeric products

$$FeCo_3H(CO)_{12} + PhC{\equiv}CPh \rightarrow FeCo_3H(CO)_9(PhC_2Ph)_2 \qquad (98)^{(63)}$$

The most extensive study was conducted with $FeRu_3H_2(CO)_{13}$ (74). This cluster reacts with diphenylacetylene to produce two isomers of $FeRu_3(CO)_{12}(PhC_2Ph)$, and these were characterized by x-ray crystallography, XXV and XXVI.

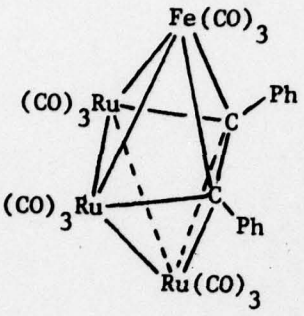

XXV

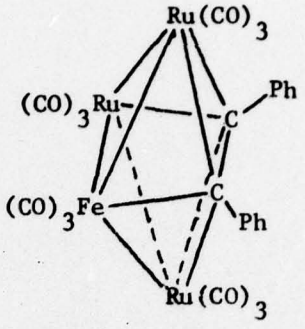

XXVI

These structures are similar to those of $Ru_4(CO)_{12}(PhC_2Ph)$ (98) and $Co_4(CO)_{10}(PhC_2Ph)$ (58) and appear to result from insertion of the alkyne across one of the metal-metal bonds. Interestingly, the two isomers XXV and XXVI slowly interconvert in refluxing hexane to give an equilibrium mixture with XXVI as the major component. With the unsymmetrical alkyne $PhC{\equiv}CMe$, three isomers of $FeRu_3(CO)_{12}(PhC_2Me)$ result.

E. Catalytic Reactions

Only a few mixed-metal clusters have been studied as homogeneous catalysts, and in all these studies the exact nature of the catalytically active species is unknown. Labroue and Poilblanc (108) reported the use of $Co_3Rh(CO)_{12}$ and $Co_2Rh_2(CO)_{12}$ as catalysts for the hydrogenation of styrene to ethylbenzene at 27°C and ~2 atm H_2. No induction period was observed, and the initial rate for $Co_2Rh_2(CO)_{12}$ was twice that for $Co_3Rh(CO)_{12}$. $Co_4(CO)_{12}$ was inactive under the same

conditions. Addition of $P(OMe)_3$ to the reaction mixture increased the rate of hydrogenation to the same magnitude as that found for $RhCl(PPh_3)_3$. Unfortunately, the reaction mixture contained unidentifiable products which were not, by comparison, simply the substituted $Co_2Rh_2(CO)_{12-n}[P(OMe)_3]_n$ (n = 1, 2, 3) clusters. A possible correlation between the catalytic and fluxional properties of these molecules was suggested (108).

Mays and coworkers (33) found that $[FeCo_3(CO)_{12}]^-$ and $FeCo_3H(CO)_{12}$ catalyze the dimerization of norbornadiene, eq. 99. The results were

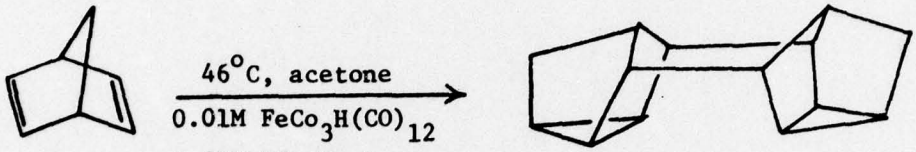

(99)

highly dependent on the solvent and the cocatalysts employed. $FeCo_3H(CO)_{12}$ was more effective than $[FeCo_3(CO)_{12}]^-$, but the nature of the actual catalytic species was not determined.

Ford and coworkers (72) have reported that several metal clusters catalyze the water gas shift reaction, eq. 100.

$$CO + H_2O \xrightarrow[FeRu_3H_2(CO)_{13},\ OH^-/diglyme]{\Delta} H_2 + CO_2 \qquad (100)$$

The most active catalyst studied was $FeRu_3H_2(CO)_{13}$, but the actual catalytic mechanism is not known. It is possible, in view of the reaction shown in eq. 89, that the reaction proceeds via one of the catalytic cycles shown in Scheme 5 (80).

Scheme V

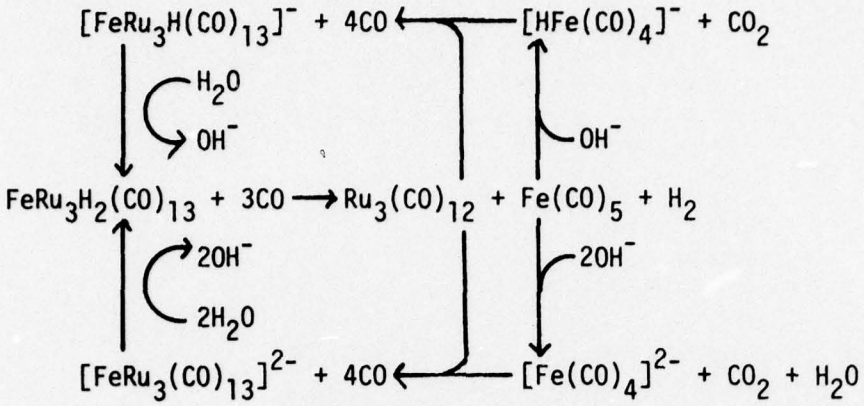

An important application of metal carbonyl clusters may come in their use as precursors for heterogeneous catalysts. In this regard, mixed-metal clusters are ideally suited for the preparation of bimetallic catalyst systems. Anderson and coworkers (17) have recently examined the absorption of clusters, including $Co_3Rh(CO)_{12}$ and $Co_2Rh_2(CO)_{12}$, onto alumina and silica. Adsorption of the clusters was more facile on alumina and was assisted by the presence of oxygen. $Co_2Rh_2(CO)_{12}$ was found to lose its bridging carbonyls upon adsorption, and further carbonyl loss occurred at temperatures >300 K. These studies also showed that upon reduction at 650°C under an H_2 atmosphere, $Co_2Rh_2(CO)_{12}$ formed a highly dispersed Co-Rh bimetallic catalyst. Importantly, this process gave a much higher degree of dispersion that could be obtained by conventional impregnation techniques using aqueous solution of $Co(NO_3)_2$ and $RhCl_3 \cdot 3H_2O$.

V. Dynamic NMR Studies

A common feature of metal clusters is their stereochemical nonrigidity in which carbonyl and hydride ligands exchange their coordination sites. Mixed-metal clusters are ideally suited for studies of the fluxional

processes in clusters because of the low symmetry which is inherent within their metal framework. In such clusters, the majority of the ligands are in chemically non-equivalent positions and thus should be distinguishable by NMR spectroscopy. The following discussion briefly describes those studies which have been conducted. The methodology has been previously discussed and will not be repeated here (7).

A. Trinuclear Clusters

Mays and coworkers (86) found that both $Fe_2Rh(Cp)(CO)_9$ and $Fe_2Co(Cp)(CO)_9$ were fluxional, but were not able to obtain a low-temperature limiting spectrum. A limiting spectrum was observed, however, with $FeRh_2(Cp)_2(CO)_6$. ^{57}Fe Mossbauer data on solid samples of this cluster had previously led (102) to assignment of the structure as XXVII, but the ^{13}C NMR spectrum at -70°C (234.5 ppm, t, 2C; 193.3 ppm, s, 2C; 190.0 ppm, s, 2C) was consistent only with structure XXVIII.

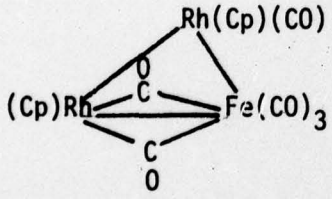

XXVII

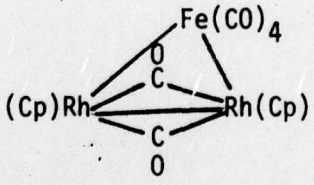

XXVIII

The triplet which was observed at room temperature agreed well with the average chemical shift calculated from the -70°C spectrum, but differed considerably in its ^{103}Rh-^{13}C coupling constant. It may be that at higher temperatures isomer XXVII is also present which could account for the increase in the average ^{103}Rh-^{13}C coupling constant.

Johnson, Lewis, and coworkers (73) examined the ^{13}C NMR spectra of a series of metal carbonyl trimers including $Fe_2Ru(CO)_{12}$ and $[MnFe_2(CO)_{12}]^-$. Each of these showed only a singlet at the lowest temperatures examined, indicating rapid exchange of the carbonyls. We have found that $Ru_2Os(CO)_{12}$ shows a 192.0 ppm singlet at room temperature which broadens upon cooling to -90°C (80). The position of the singlet agrees very well with the chemical shift calculated from a weighted average of the singlets observed in the spectra of $Ru_3(CO)_{12}$ (198 ppm, 25°C) and $Os_3(CO)_{12}$ (178.1 ppm, 156°C).

Aime and coworkers (9) studied the ^{13}C NMR spectra of $FeCo_2(CO)_9S$ and several of its phosphine derivatives. At -115°C, $FeCo_2(CO)_9S$ exhibits three peaks in a 1:2:6 intensity ratio. The large peak was attributed to the Co-CO's which were undergoing rapid scrambling. At -65°C, the Fe-CO's undergo localized scrambling on the Fe atom, and above this temperature, all of the carbonyls become equivalent. The ^{13}C NMR spectra of the substituted $FeCo_2(CO)_{9-n}S(L)_n$ (n = 1-3) derivatives indicated that the first two phosphines bind successively to the Co atoms, while the third phosphine binds to Fe. Although this study indicated that the phosphines all substitute within the equatorial $FeCo_2$ plane, it was not possible to assign the absolute stereochemistry. For instance, both XXIX and XXX are possible structures for the monosubstituted derivative.

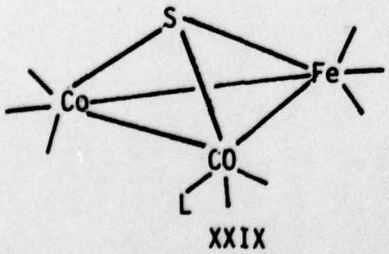

XXIX

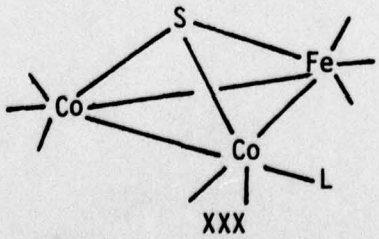

XXX

These $FeCo_2(CO)_{9-n}S(L)_n$ (n = 1-3) clusters are fluxional on the NMR time scale (9). In each case, localized exchange first occurs on the unsubstituted Co atom and then localized exchange occurs on Fe. Finally, exchange of all the carbonyls occurs to yield only a single resonance in the high temperature spectrum. Line-shape analysis led to the following order of activation energies for exchange of the carbonyls bound to iron:

$$FeCo_2(CO)_7[P(n\text{-}Bu)_3]_2 > FeCo_2(CO)_8[P(n\text{-}Bu)_3] > FeCo_2(CO)_8[P(OPh)_3] > FeCo_2(CO)_9S$$

It was suggested that an increase in the electron density on the cluster due to substitution weakens the metal-metal bonds and thereby facilitates scrambling within the $Fe(CO)_3$ fragment (9). The mechanism of carbonyl exchange between the metals remains unclear.

B. Tetranuclear Clusters

$Co_3Rh(CO)_{12}$ exhibits a ^{13}C spectrum at -85°C consistent with structure XXXI (97). At this temperature, the carbonyls bound to the unique cobalt

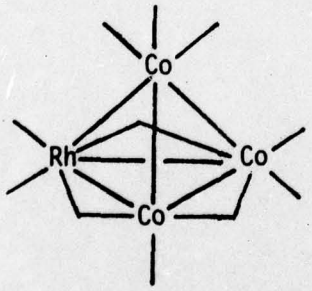

XXXI

give rise to a single resonance indicating they are rapidly interchanging. The next process (T_c = -45°C) involves interchange of the carbonyls on the three $RhCo_2$ faces. The Rh is always maintained in the basal triangle in this process although the bridging carbonyls exchange positions, Scheme VI. At temperatures greater than -30°C, all the carbonyls become equivalent. The

Scheme VI

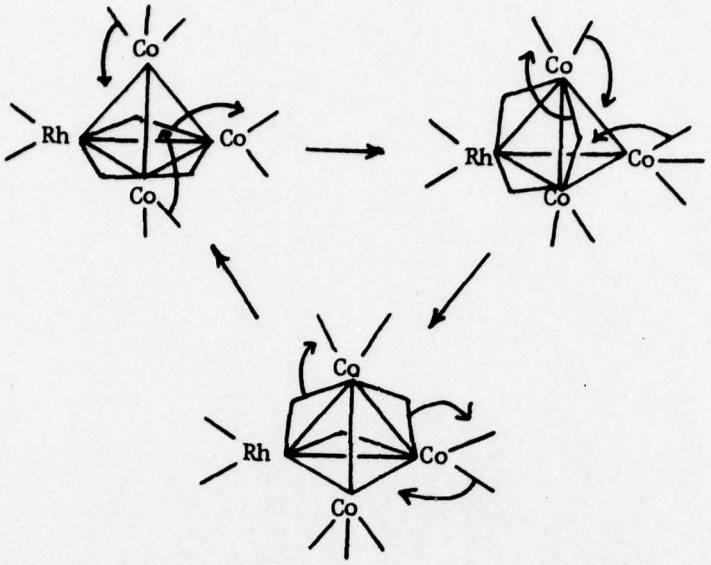

mechanism for this last process probably involves a tetrahedral intermediate similar to that proposed by Cotton et al. (56) to explain the fluxionality of $Rh_4(CO)_{12}$.

Milone and coworkers (8) examined the ^{13}C spectra of $FeCo_3H(CO)_{12}$, XXXII and some of its substituted derivatives. At -89°C, two resonances

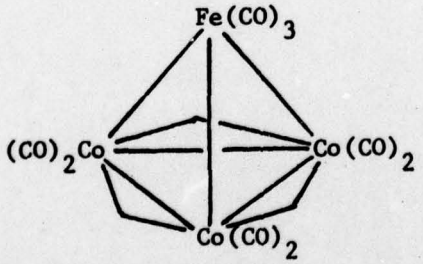

XXXII

in a 1:2 ratio were observed in the spectrum of $FeCo_3H(CO)_{12}$. As the temperature was raised, the furthest upfield and more intense peak broadened significantly. It was assumed that the cobalt carbonyls were

rapidly exchanging at -85°C, and this peak was attributed to an average cobalt-carbonyl resonance which broadens at room temperature due to coupling to ^{59}Co. The second resonance was attributed to rapidly exchanging Fe carbonyls. The observed disparity of intensities (1:2 observed, 1:3 expected) is similar to that found for the isoelectronic $Co_4(CO)_{12}$.

The substituted $FeCo_3H(CO)_{12-n}(L)_n$ (n = 1-3) derivatives (8) all yielded spectra consistent with the proposed or proven structures XXXIII, XXXIV, and XXXV. Increasing substitution slowed the exchange processes within the Co_3 triangle. Arguments were given to the effect that substitution of a carbonyl with a phosphine ligand increased the electron density on the cluster and this in turn increased the need for the bridging carbonyls as an effective means of removing the excess electron density. Since the transitional state in the fluxional process would involve

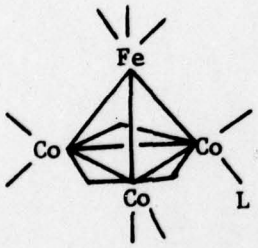

XXXIII

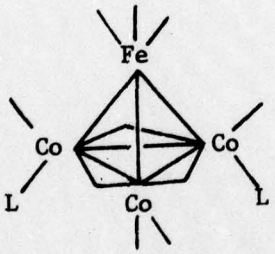

XXXIV

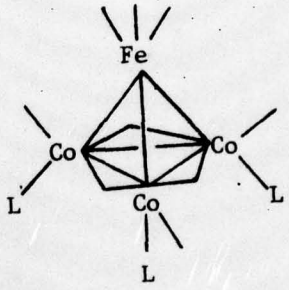

XXXV

breaking the carbonyl bridges, the activation barrier should therefore increase.

We have studied the dynamic properties of $FeRu_3H_2(CO)_{13}$, $FeRu_2OsH_2(CO)_{13}$, and $FeRuOs_2H_2(CO)_{13}$ (77). The structure of $FeRu_3H_2(CO)_{13}$, was determined by x-ray crystallography (79), and $FeRu_2OsH_2(CO)_{13}$, and $FeRuOs_2H_2(CO)_{13}$ were assumed to have similar structures on the basis of

their infrared, electronic absorption, and NMR spectral data (78). The mechanisms of CO exchange were found by ^{13}C NMR spectroscopy to be identical for these three clusters, and our further discussion will involve only $FeRuOs_2H_2(CO)_{13}$. This cluster exists in the two isomeric forms shown below with their C_s and C_1 symmetry labels. The low temperature

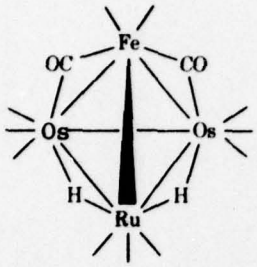

C_s

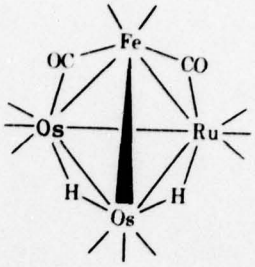

C_1

limiting ^{13}C NMR spectrum of the mixture of these isomers is shown in Figure 6. Nineteen of the twenty-one chemically non-equivalent carbonyls present in the isomeric mixture are clearly observable in the ^{13}C NMR spectrum, illustrating the utility of mixed-metal clusters in studies of this type. Three basic exchange processes occur in these clusters as the temperature is raised from -60° to 100°C. The first process involves exchange of the bridging and terminal carbonyls bound to iron (C_1, T_c = -40°C ; C_s, T_c = -20°C). In the second process eight carbonyls execute a cyclic motion around the Fe-M-M triangle that initially contained the bridging carbonyls (C_1, T_c = -20°C ; C_s, T_c = 20°C). The third process manifests itself in two distinct ways, Scheme VII. First, the two enantiomers of the C_1 isomer interconvert. This occurs by a shift in the metal framework in which the Fe moves away from Os_A and towards Os_B concerted with movement of the hydride

that bridges the Os_A-Ru bond to a position bridging the Os_B-Ru bond.

Scheme VIII

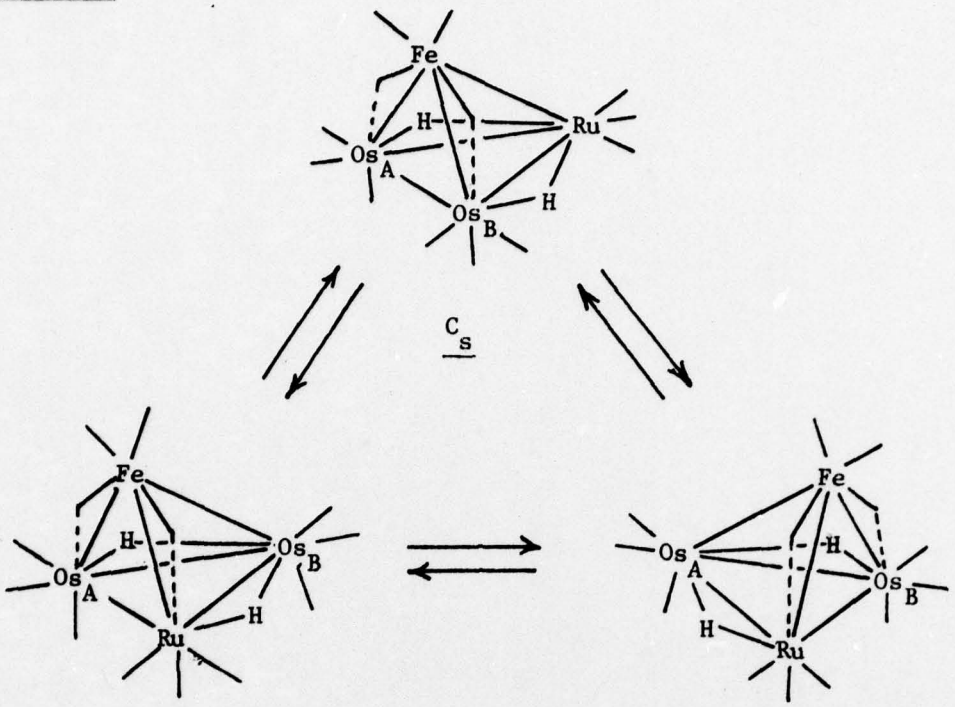

Finally, in the last process, the Fe moves away from Ru and towards Os_A to give the C_s isomer. The interconversion of the three faces of the cluster which possess the bridging carbonyls coupled with the cyclic exchange process about each of these faces leads to total exchange of all the carbonyls in the cluster. The activation barriers for each of the three exchange processes (bridge exchange, cyclic exchange, metal shift) was observed to increase in the order $FeRu_3H_2(CO)_{13}$ < $FeRu_2OsH_2(CO)_{13}$ < $FeRuOs_2H_2(CO)_{13}$.

In a separate study ^1H, ^{31}P and ^{13}C NMR were used to show that $FeRu_3H_2(CO)_{12}(PMe_2Ph)$ exists in the two isomeric forms XXXVI and XXXVII (82).

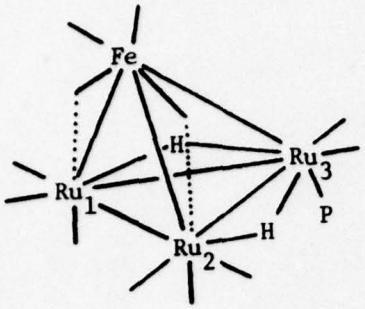

C_s

XXXVI

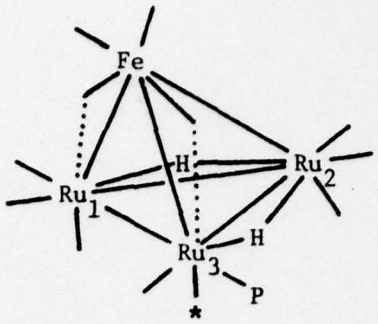

C_1

XXXVII

An alternate substitution site in the C_1 isomer that was also consistent with the NMR data is indicated by the asterisk. Complete assignment of the ^{13}C NMR spectrum of the compound was not possible because of overlapping resonances, but much information was extracted from the ^1H NMR spectrum. These two isomers were found to interconvert, presumably by the same type of intrametallic rearrangment process discussed above.

Perhaps of greater importance was comparison of the series of $FeRu_3H_2(CO)_{12}L$ clusters in which L = $P(OMe)_3$, $P(OEt)_2Ph$, PPh_3, $PMePh_2$, PEt_2Ph, PMe_2Ph, PMe_3, and $P(\underline{i}\text{-}Pr)_3$ (82). A comparison of the $C_s \rightleftarrows C_1$ equilibrium constants with the cone angle and basicity of the phosphorous ligand for the various derivatives in hexane solution is shown in Table II. No correlation was found using only size or basicity alone and both factors affect the position of this equilibrium. With large ligands, the cluster exists totally as the C_s isomer, regardless of ligand basicity. With smaller ligands, the complex may exist as both isomers but with the C_1 isomer increasing in stability as the basicity of the phosphorous donor ligand increases. The equilibrium was found to be quite solvent dependent and more polar solvents favored the C_s isomer.

The solid state structure of $Ru_3CoH_3(CO)_{12}$ was shown by x-ray crystallography to have C_{3v} symmetry, XXXVIII (81).

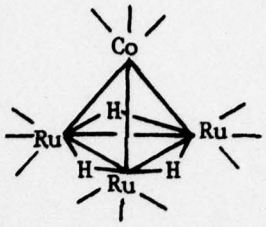

XXXVIII

However, infrared and ^1H NMR spectroscopy showed that more than one isomer of this cluster exists in solution. The C_{3v} structure XXXVIII has no bridging carbonyls but the infrared spectrum of the cluster in hexane solution showed a ν_{CO} at 1878 cm^{-1}. ^1H NMR measurements at -100°C confirmed the presence of two isomers and showed that the second isomer contained three nonequivalent hydrogens. Structure XXXIX was suggested for the second isomer. At elevated temperatures these isomers interconvert (T_C = -40°C).

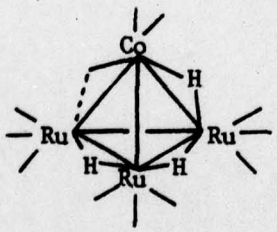

XXXIX

VI. Almost Mixed-Metal Clusters

Because of the requirements we set at the beginning concerning the scope of this review, we have had to exclude several interesting compounds. Since these may be of interest to some readers, they are briefly mentioned here, although this section is not meant to be comprehensive.

A number of linear mixed-metal carbonyls are known. Sheline and coworkers prepared a series of M-Fe-M (M = Tc, Re) trimers by photolysis of $Fe(CO)_5$ and the corresponding $M_2(CO)_{10}$, eq. 101 (66,109).

$$M_2(CO)_{10} + Fe(CO)_5 \xrightarrow{h\nu} (CO)_5\,M\text{-}Fe(CO)_4\text{-}M(CO)_5 \qquad (101)$$

(M = Mn, Tc, Re)

Schmid and coworkers (136) have prepared several derivatives which possess the $[Co_3(CO)_{10}]^-$ unit as an oxygen donor ligand to another metal. Reactions 102-105 are illustrative.

$$7Co_2(CO)_8 + 4Ti(Cp)_2Cl_2 \longrightarrow 4\ \text{[cluster]} + CoCl_2 + 16CO \qquad (102)$$

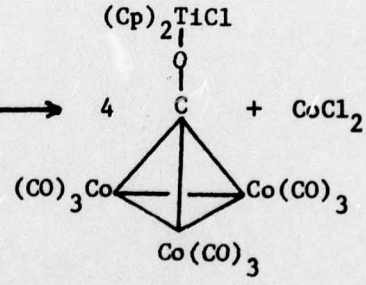

(138)

$$2[Co_3(CO)_{10}]^- + M(Cp)_2Cl_2 \longrightarrow \text{[cluster]} \qquad (103)$$

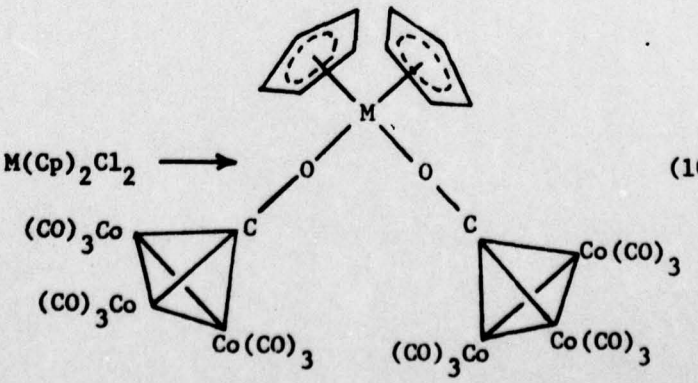

(152)

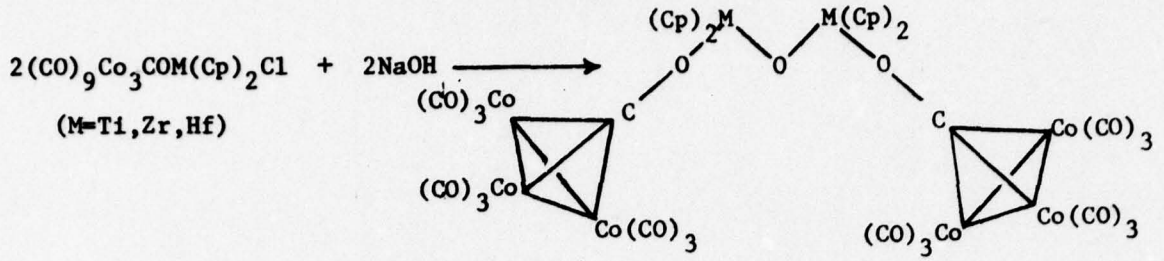

(152)

(104)

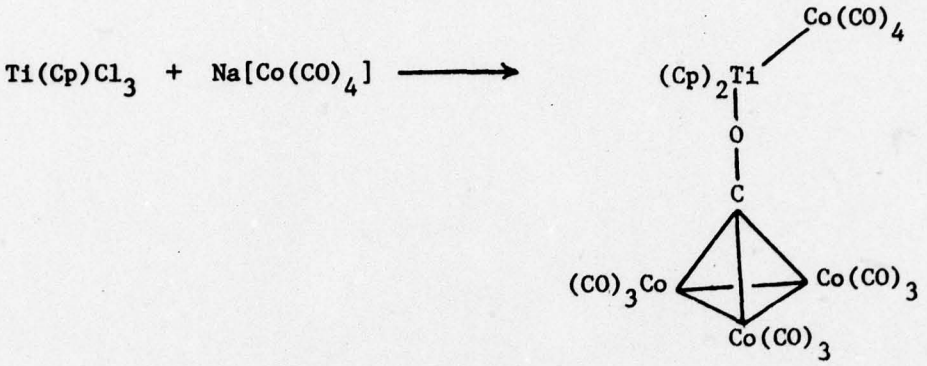

(139)

(105)

Mason and coworkers (83,84,114) prepared $[Fe_2Rh(Cp)_2(CO)_2(PPh_2)_2]^+$ XXXX by the reaction shown in eq. 106.

$$[Rh(CO)_2Cl]_2 + \text{excess } Ph_2P\text{-}Fe(Cp)(CO)_2 \xrightarrow{MeOH} [Fe_2Rh(Cp)_2(CO)_4(PPh_2)_2]^+ \quad (106)$$

XXXX

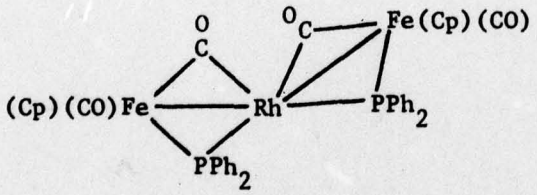

XXXX

Norton and coworkers (5,6) developed an improved synthetic method for this trimer and they prepared the Ru_2Ir and Fe_2Ir analogues. These compounds undergo racemization on the NMR time scale with free energies of

activation of 12.6, 17.5, and 17.8 kcal/mole for the Fe_2Rh, Fe_2Ir, and Ru_2Ir complexes, respectively.

$HMnRe_2(CO)_{14}$, XXXXI, was shown to have a "bent" disposition of metals with the hydride lying between the Re atoms (44,69).

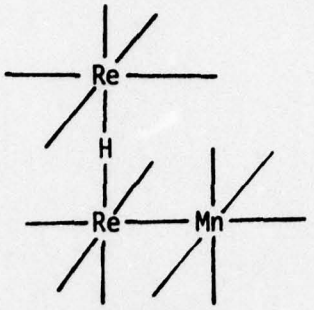

XXXXI

Dahl and coworkers prepared the unusual compound $Mo_2Re_2(Cp)_2(CO)_{12}(S)_2$, XXXXII, containing both tri- and tetracoordinated sulfur ligands, eq. 107 (158).

$$[Re(CO)_4SSnMe_3]_2 + Mo(Cp)(CO)_3Cl \xrightarrow[\text{benzene}]{75°C} Mo_2Re_2(Cp)_2(CO)_{11}(S)_2 \quad (107)$$

XXXXII

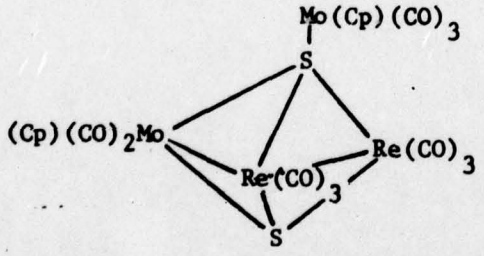

XXXXII

Chini and coworkers (42) found that $[Co(CO)_4]^-$ reacts with CuI and AgI to give high yields of $[(CO)_4CoCuCo(CO)_4]^-$ and $[(CO)_4CoAgCo(CO)_4]^-$ of structure XXXXIII. The copper complex is less stable than the silver species and readily dissociates in CH_3CN. Reaction 108, however, is

$$(CO)_4Co-M-Co(CO)_4^-$$

XXXXIII

reversible and the starting material can be recovered after solvent removal.

$$\{Cu[Co(CO)_4]_2\} + nCH_3CN \rightleftarrows [Cu(CH_3CN)_n]^+ + 2[Co(CO)_4]^- \qquad (108)$$

$Rh_2Ag(PPh_3)_3[C_2(C_6F_5)]_5$, XXXXIV, has been prepared by a reaction similar to that which gave $Ir_2Cu_4(PPh_3)_2(C_2Ph)_8$ (4,46). The structure shows octahedral Rh coordination and tetrahedral Ag coordination. The 3.1 Å Rh-Ag distances indicate that little metal-metal bonding exists.

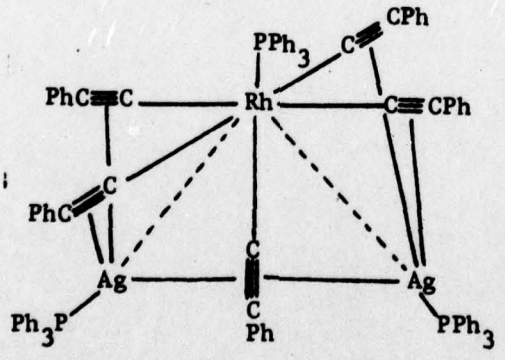

XXXXIV

Acknowledgment. We are most grateful to Professors P. Braunstein, P. Chini, L. Milone, J. Shapley, and F. G. A. Stone for providing preprints of their work prior to publication and to Elizabeth Gladfelter and Carla Hofland for assistance in preparation of the manuscript. Our own research described herein was supported in part by the Office of Naval Research.

Table I. Mixed-Metal Clusters

Index No.	Cluster[a]	Color	ν_{CO}[b]	Other Available Spectral Data[c]	Crystal Structure	References
Titanium:						
1.	$TiCo_2(Cp)_2(CO)_8$	---	----	----	No	140
Zirconium:						
2.	$Zr_2Co_2(Cp)_4(CO)_5$	----	----	----	No	140
Vanadium:						
3.	$VCo_3(Cp)(CO)_9$	black-brown	pentane: 2086 w, 2063 s, 2054 s, 2025 m, 1864 m	Mass	No	85
Tantalum:						
4.	$[(Ta_4Mo_2Cl_{12})Cl_6]^{2-}$	dark green	----	UV-VIS, far-ir, mag, ESR	No	117
5.	$[(Ta_5MoCl_{12})Cl_6]^{2-,3-}$	dark red	---	UV-VIS, far-ir, mag	No	117
Chromium:						
6.	$CrPt_2\{\mu\text{-}C(OMe)Ph\}(CO)_6L_2$ L = $PMe(t\text{-}Bu)_2$, PCy_3	red	L = $PMe(t\text{-}Bu)_2$: 2019 vs, 1936 vs, 1908 vs, br, 1876 m	^1H, ^{31}P	No	18

Table I. (continued)

Index No.	Cluster[a]	Color	ν_{CO}[b]	Other Available Spectral Data[c]	Crystal Structure	Reference(s)
7.	$CrFe_2(CO)_{11}(PPh)$	deep red	hexane: 2083 w, 2057 w, 2036 vs, 2024 vs, 2016 s, 1982 m, 1968 w, 1945 w, 1938 m,	Mass, ^1H	Yes	93
8.	$CrFeCo_2(CO)_{14}S$	black	cyclohexane: 2108 w, 2071 m, 2059 s, 2040 m, 2033 w, 1989 m, 1963 s	----	Yes	132
9.	$[Cr_2Ni_3(CO)_{16}]^{2-}$	dark red	CH_2Cl_2: 2040 w, 1982 s, 1925 w, 1890 m, 1942 mw, 1795 w	----	Yes	134
Molybdenum: (see also entries 4 and 5)						
10.	$Mo_2Fe(Cp)_2(CO)_8$	red	pentane: 2050, 2020, 2000, 1900, 1875	^1H	No	57
11.	$Mo_2Pt(Cp)_2(CO)_4(PPh_3)_2$	red	pentane: 1980, 1808	^1H	No	57
12.	$MoOs_3H(Cp)(CO)_{12}$	----	----	----	No	48
13.	$MoOs_3H_3(Cp)(CO)_{11}$	----	----	----	No	48
14.	$MoCo_3(Cp)(CO)_{11}$	black	CCl_4: 2092 s, 2052 vs, 2045 vs, 2034 s, 1996 s, 1982 m, 1956 s, 1887 w, 1861 m, 1835 sh	^1H, Mass	Yes	137
15.	$[Mo_2Fe_2(Cp)_2(CO)_{10}]^{2-}$	maroon	CH_2Cl_2: 1998 ms, 1932 vs, 1884 vs, 1868 ms (sh)	^1H	No	88

Table I. (continued)

Index No.	Cluster[a]	Color	ν_{CO}[b]	Other Available Spectral Data[c]	Crystal Structure	Reference(s)
16.	$[Mo_2Ni_4(CO)_{14}]^{2-}$	----	----	----	Yes	134
17.	$Mo_2Pd_2(Cp)_2(CO)_6L_2$ L = PPh_3, PEt_3	violet	KBr: 1842 vs, 1801 m, 1772 vs	^1H	Yes	21,60
18.	$Mo_2Pt_2(Cp)_2(CO)_6(PPh_3)_2$	black	KBr: 1831 vs, 1805 w (sh), 1741 vs	----	No	26
19.	$[Mo_2Ni_3(CO)_{16}]^{2-}$	red-orange	CH_2Cl_2: 2039 w, 1994 s, 1933 m, 1901 s, 1838 w, 1786 w		Yes	134
Tungsten:						
20.	$WPt_2\{\mu\text{-}C(OMe)Ph\}(CO)_6L_2$ L = $PMe(t\text{-}Bu)_2$, PCy_3	red	cyclohexane, L = $PMe(t\text{-}Bu)_2$: 2032 s, 1940 m, 1922 s, 1941 (sh)	^1H, ^{31}P ^{13}C	Yes	18
21.	$W_2Ni(\mu\text{-}CC_6H_4CH_3)_2(Cp)_2(CO)_4$	purple	----	----	No	19
22.	$W_2Pd(\mu\text{-}CC_6H_4CH_3)_2(Cp)_2(CO)_4$	purple	----	----	No	19
23.	$W_2Pt(\mu\text{-}CC_6H_4CH_3)_2(Cp)_2(CO)_4$	purple	----	----	No	19
24.	$WRu_3H(Cp)(CO)_{12}$	----	----	----	No	48
25.	$WOs_3H(Cp)(CO)_{12}$	red	----	^1H	Yes	48
26.	$WOs_3H_3(Cp)(CO)_{11}$	orange	----	^1H	Yes	48
27.	$WCo_3(Cp)(CO)_{11}$	black	CCl_4: 2090 s, 2052 vs, 2045 vs, 2034 s, 1994 s, 1976 m, 1944 s, 1885 w, 1859 m, 1832 s	^1H	No	137

Table I. (continued)

Index No.	Cluster[a]	Color	ν_{CO}[b]	Other Available Spectral Data	Crystal Structure	Reference(s)
28.	$[W_2Fe_2(Cp)_2(CO)_{10}]^{2-}$	red-violet	CH_2Cl_2: 1997 w, 1930 ms, 1880 m (br)	^1H	No	88
29.	$[W_2Ni_3(CO)_{16}]^{2-}$	orange	CH_2Cl_2: 2036 w, 1998 s, 1930 mw, 1896 s, 1835 m, 1791 w	----	Yes	134
Manganese:						
30.	$[MnFe_2(CO)_{12}]^-$	blue-black	THF: 2063, 1999, 1990, 1972, 1944, 1903, 1827, 1785	UV, ^{13}C	No	15,73
31.	$[MnFe_2(CO)_{11}L]^-$ L = PPh_3, $PMePh_2$, $P(O\text{-}\underline{i}\text{-}Pr)_3$	dark green	THF, L = PPh_3: 2040 m, 1997 w (sh), 1974 s, 1953 s, 1927 m, 1887 w, 1785 w, 1750 w	Moss, ^1H	No	53
32.	$MnFe_2(Cp)(CO)_8(PPh)$	deep red	----	----	Yes	91,92
33.	$[MnOs_2(CO)_{12}]^-$	red	THF: 2080 w, 2018 s, 1981 vs, 1943 m, 1914 m 1897 sh, 1887 m	----	No	106
34.	$MnOs_2H(CO)_{12}$	orange	hexane: 2136 w, 2081 s, 2051 vs, 2038 vs, 2016 m, 2001 m, 1993 m, 1975 m, 1957 m, 1951 m	Mass	No	106
35.	$[MnNi_2(Cp)_2(CO)_5]^-$	green-black	THF: 1971 vs, 1896 s, 1878 s (sh), 1744 w, 1688 m, 1647 w (sh)	^1H	No	87

Table I. (continued)

Index No.	Cluster[a]	Color	ν_{CO}[b]	Other Available Spectral Data[c]	Crystal Structure	Reference(s)
36.	$MnOs_3H(CO)_{16}$	yellow	hexane: 2136 w, 2093 m, 2069 s, 2056 s, 2031 m, 2022 m, 2015 m, 2006 m, 1996 m, 1988 m (br), 1977 m, 1970 w	Mass	No	106
37.	$MnOs_3H_3(CO)_{13}$	scarlet	KBr: 2133 m, 2086 s, 2055 s, 2043 sh, 2020 sh, 1990 sh, 1950 m, 1830 m	----	No	106
Technetium:						
38.	$[TcFe_2(CO)_{12}]^-$	dark red	THF: 2077 w, 2008 w, 1987 s, 1943 m, 1903 w, 1815 w, 1783 w	----	No	109
Rhenium:						
39.	$[ReFe_2(CO)_{12}]^-$	yellow	THF: 2075 w, 2006 m, 1991 s, 1946 m, 1903 w, 1814 w, 1785 w	----	No	66
40.	$[ReOs_2(CO)_{12}]^-$	orange	THF: 2085 w, 2021 s, 2009 s, 1990 s, 1945 w, 1941 sh, 1925 sh, 1887 m	----	No	106
41.	$ReOs_2H(CO)_{12}$	yellow	hexane: 2136 w, 2086 s, 2058 sh, 2053 vs, 2029 m, 2014 m, 2000 s, 1992 m, 1982 m, 1967 m, 1953 m	Mass	No	106

Table 1. (continued)

Index No.	Cluster[a]	Color	ν_{CO}[b]	Other Available Spectral Data[c]	Crystal Structure	Reference(s)
42.	$Re_2RuH_2(CO)_{12}$	yellow	hexane: 2095 m, 2091 sh, 2070 m, 2042 s, 2034 sh, 2009 m, 2001 m, 1987 m, 1978 m, 1956 m	----	No	106
43.	$Re_2PtH_2(CO)_9(PPh_3)$	----	----	----	No	149
44.	$Re_2AuH(CO)_9(PPh_3)$	----	----	----	No	149
45.	$[ReRu_3(CO)_{16}]^-$	orange-red	THF: 2009 vs, 1982 s, 1960 (br) sh, 1932 sh, 1891 m	----	No	106
46.	$ReOs_3H(CO)_{15}$	orange	KBr: 2131 w, 2091 s, 2070 sh, 2057 sh, 2051 s, 2018 s, 1991 sh, 1971 sh, 1950 m, 1933 m	Mass	Yes	47,106
47.	$ReOs_3H(CO)_{15}(NCCH_3)$	----	C_6H_{12}: 2114 vw, 2084 m, 2058 m, 2029 m, 2015 sh, 2002 s, 1991 m, 1981 w, 1971 m, 1965 sh, 1932 w	Mass	No	142,143
48.	$ReOs_3H_3(CO)_{13}$	orange	KBr: 2138 s, 2090 s, 2063 sh, 2030 br, 1983 s, 1968 sh, 1900 m	----	No	106
49.	$ReOs_3H(CO)_{16}$	yellow	----	^1H, Mass	No	47,106
50.	$ReOs_3H_5(CO)_{12}$	----	----	----	No	106
51.	$Re_2Ru_2H_2(CO)_{16}$	yellow	----	----	No	106

Table I. (continued)

Index No.	Cluster[a]	Color	ν_{CO}[b]	Other Available Spectral Data[c]	Crystal Structure	Reference(s)
52.	$Re_2Os_3H_2(CO)_{16}$	----	----	----	No	143
53.	$Re_2Os_3H_2(CO)_{19}$	----	C_6H_{12}: 2107 m, 2078 m, 2062 m, 2051 m, 2015 s, 2004 s, 2000 s, 1994 s, 1984 m, 1976 s, 1964 s, 1950 vw, 1930 w	^1H, Mass	No	144
54.	$Re_2Os_3H_2(CO)_{20}$	yellow	----	^1H, ^{13}C, Mass	Yes	144
Iron: (see also entries 7, 8, 10, 15, 28, 30-32, 38 and 39)						
55.	$FeRu_2(CO)_{12}$	orange-red	cyclohexane: 2067 s, 2042 vs, 2034 s, 2012 w, 1988 w	UV-VIS, Mass	No	161
56.	$FeOs_2(CO)_{12}$	orange	heptane: 2070 s, 2042 vs, 2034 vs, 2022 m, 2008 w, 2003 m, 1988 w	----	No	121
57.	$FeCo_2(CO)_9Y$ Y = S, Se, Te	violet	hexane, Y = S: 2104 vw, 2066 s, 2054 vs, 2042 s, 2029 m, 2000 vw, 1985 m, 1950 vw	^{13}C	Yes	99,148,151
58.	$FeCo_2(CO)_9(PPh)$	black	light petroleum: 2101 w, 2059 vs, 2048 vs, 2039 vs, 1981 w, 1969 w	Mass	No	23
59.	$FeCo_2(CO)_8(L)S$ L = PPh_3, $AsPh_3$, $P(OEt)_3$, PEt_2Ph, $P(n\text{-}Bu)_3$	red-brown	hexane, L = PPh_3: 2080 m, 2038 s, 2031 (sh), 2027 m, 2017 m, 1986 w, br, 1966 w, br, 1949 vw	Moss, ^1H, ^{13}C	No	31,133

Table I. (continued)

Index No.	Cluster[a]	Color	ν_{CO}[b]	Other Available Spectral Data[c]	Crystal Structure	Reference(s)
60.	$FeCo_2(CO)_7(L)_2S$ L = PPh_3, $P(n\text{-}Bu)_3$, PEt_2Ph, $CNC(CH_3)_3$	dark green or red	hexane, L = $CNC(CH_3)_3$: 2020 vs, 2006 s, 1999 m, 1984 m, 1948 m	Moss, ^1H ^{13}C	No	31,126,133
61.	$FeCo_2(CO)_6(L)_3S$ L = PPh_3, $P(n\text{-}Bu)_3$, $CNC(CH_3)_3$	red	hexane, L = $CNC(CH_3)_3$: 2002 vs, 1996 s, 1983 s, 1970 m, 1931 m, 1864 vw, 1831 w, 1823 w	^1H, ^{13}C	No	126,133
62.	$FeCo_2H(CO)_9(CR)$ R = CH_3, C_2H_5, C_6H_5	maroon	hexane, R = CH_3: 2101 m, 2065 m, 2053 s, 2047 s, 2037 s, 2018 m, 2014 m, 1994 w, 1989 m	UV-VIS, Mass ^1H	No	64
63.	$FeCo_2(CO)_8(PhC_2Ph)$	----	----	Mass	No	53
64.	$FeRh_2(Cp)_2(CO)_6$	green	2054 s, 2002 s, 1989 s, 1980 s, 1839 w, 1792 m	^1H, ^{13}C Moss	No	86,102
65.	$FeNi_2(Cp)_2(CO)_5$	green-black	hexane: 2050 vs, 2004 s, 1983 s, 1823 vw, 1790 w, 1762 m	Moss	Yes	87,154
66.	$FeNi_2(Cp)_2(CO)_3(PhC_2R)$ R = H, Ph, C_2Ph	black	R = Ph: 2043, 1967	^1H	No	155
67.	$FePt_2(CO)_5[P(OPh)_3]_3$	orange	cyclohexane: 2032 sh, 2015 s, 1952 m, 1918 m	----	Yes	29,11,12
68.	$Fe_2Ru(CO)_{12}$	purple	cyclohexane: 2057 s, 2044 vs, 2023 w (sh), 2044 m (br), 1859 vvw, 1834 vvw	Mass, ^{13}C UV-VIS	No	161

Table I. (continued)

Index No.	Cluster[a]	Color	ν_{CO}[b]	Other Available Spectral Data[c]	Crystal Structure	Reference(s)
69.	$Fe_2Ru(Cp)(CO)_6(PPh_3)(C_2Ph)$	dark red	2066 s, 2049 s, 2022 w, 2007 sh, 1974 s (br), 1944 vw	Mass	No	1,27
70.	$Fe_2Os(CO)_{12}$	purple	hexane: 2117 w, 2055 s, 2041 s, 2036 s, 2013 m, 2001 m, 1990 sh, 1860 vw, 1827 vw	----	No	104,121
71.	$Fe_2Co(Cp)(CO)_9$	brown	2080 s, 2033 s, 2013 s, 2001 sh, 1981 m, 1848 w, 1812 m	^1H, ^{13}C, Moss	No	86,102
72.	$Fe_2CoH_2(CO)_9CR$ R = H, CH_3, C_2H_5, C_3H_7	pink	hexane: 2101 m, 2054 vs, 2047 vs, 2038 s, 2017 m, 1988 m, 1985 m	----	No	64
73.	$Fe_2Rh(Cp)(CO)_9$	green	2079 s, 2037 s, 2032 sh, 2015 s, 1999 s, 1982 sh, 1844 w, 1803 m	^1H, ^{13}C, Moss	No	86,102
74.	$Fe_2Ni(Cp)(CO)_7(CEt)$	grey-violet	heptane: 2070 s, 2036 vs, 2012 s, 1986 m, 1974 m, 1954 mw	^1H, Moss	No	118
75.	$Fe_2Ni(Cp)(CO)_6(C_2Me)$	grey-violet	heptane: 2060 s, 2020 vs, 1990 s, 1982 s (sh), 1968 m	^1H, Moss	No	118
76.	$Fe_2Pt(CO)_9L$ L = PPh_3, $PMePh_2$, PMe_2Ph, $AsPh_3$, PMe_3	deep red	cyclohexane, L = PPh_3: 2074 s, 2035 s, 2014 s, 2001 m, 1985 s, 1973 (sh), 1924 w, br	^1H	Yes	28,29,115

Table I. (continued)

Index No.	Cluster[a]	Color	ν_{CO}[b]	Other Available Spectral Data[c]	Crystal Structure	Reference(s)
77.	$Fe_2Pt(CO)_8L_2$ L = $PMePh_2$, PMe_2Ph, $P(OMe)_2Ph$, $P(OPh)_3$, dppe, diars	deep red	cyclohexane, L = PMe_2Ph: 2051 s, 1998 s, 1971 m, 1948 m, 1892 w, br	^1H	No	28,29,43
78.	$FeRuOs_2H_2(CO)_{13}$	orange	hexane: 2121 w, 2086 s, 2073 s, 2041 vs, 2032 m, 2024 m, 2013 w, 1993 m	^1H, ^{13}C, UV-VIS, Mass	No	77,78
79.	$FeRu_2OsH_2(CO)_{13}$	orange-red	hexane: 2111 vw, 2085 s, 2073 s, 2041 vs, 2026 m, 2016 w, 1991 m, 1887 w, 1877 w, 1861 m, 1849 m	^1H, UV-VIS Mass	No	78
80.	$[FeRu_2Co(CO)_{13}]^-$	red-brown	CH_2Cl_2: 2072 w, 2028 s, 2008 vs, 1195 s (sh), 1950 m (sh), 1826 w (sh), 1795 m, br	----	No	147
81.	$[FeRu_3H(CO)_{13}]^-$	black	CH_2Cl_2: 2073 w, 2031 s, 2013 s, 1998 s, 1974 m, 1944 m, 1840 w, 1811 m	----	No	80
82.	$FeRu_3H_2(CO)_{13}$	red	cyclohexane: 2112 vvw, 2084 vs, 2073 vs, 2063 w, 2041 vs, 2031 m, 2021 w, 1992 m, 1884 w, 1845 m	^1H, ^{13}C UV-VIS	Yes	77-79,101, 119,161
83.	$FeRu_3H_2(CO)_{12}L$ L = $P(OMe)_3$, $P(OEt)_2Ph$, PPh_3, $PMePh_2$, PEt_2Ph, PMe_2Ph, PMe_3, $P(i\text{-}Pr)_3$	dark red	hexane, L = PMe_2Ph: 2096 s, 2072 s, 2064 s, 2046 s, 2034 (sh), 2028 s, 2020 s, 2012 m, 1990 m, 1984 m, 1876 w, 1850 m, 1806 m	^1H	No	82

Table I. (continued)

Index No.	Cluster[a]	Color	ν_{CO}[b]	Other Available Spectral Data[c]	Crystal Structure	Reference(s)
84.	$FeRu_3(CO)_{12}(RC_2R')$ R,R' = Ph (2 isomers) R,R' = CH_3 (2 isomers) R = Ph, R' = CH_3 (3 isomers)	brown, red-brown	hexane, R,R' = Ph, isomer I: 2095 m, 2064 s, 2049 s, 2036 s, 2024 m, 2016 m, 1998 m, 1986 w, 1976 w, 1962 vw	^1H, Mass	Yes	74
85.	$FeRu_3H_4(CO)_{12}$	orange	cyclohexane: 2085 s, 2070 s, 2054 s, 2044 vw, 2031 m (br), 2012 w, 1998 w, 1990 w	^1H	No	107
86.	$FeOs_3H_2(CO)_{13}$	orange	heptane: 2086 s, 2072 s, 2040 vs, 2032 m, 2025 m, 2015 w, 1994 w, 1875 w, 1848 m	----	No	121
87.	$FeCo_3H(CO)_{12}$	purple	hexane: 2059 s, 2050 s, 2026 m, 1986 m, 1885 m	UV-VIS, Mass, ^{13}C	No	8,35,39,64, 103,116
88.	$FeCo_3H(CO)_{11}L$ L = $PMePh_2$, PEt_3, $P(OPr)_3$, $P(OPh)_3$, $P(OMe)_3$, PPh_3	purple	hexane, L = $PMePh_2$: 2076 m, 2040 s, 2031 vs, 2008 s, 1996 m (sh), 1970 m, 1935 vw, 1891 w, 1865 m, 1846 m	^1H, Mass, Moss, ^{13}C	No	8,54,89
89.	$FeCo_3H(CO)_{10}L_2$ L = $PMePh_2$, PPh_3, PEt_3, $P(OPh)_3$, $P(OPr)_3$, $P(OMe)_3$ L_2 = dppe	blue-green	$CHCl_3$, L = $PMePh_2$: 2050 vs, 2017 vs, 1991 vs, 1951 m (sh), 1866 w (sh), 1826 m (br)	^1H, Moss, ^{13}C	No	8,54,89
90.	$FeCo_3H(CO)_9L_3$ L = $PMePh_2$, $P(OMe)_3$ L_3 = 3/2 dppe	green	cyclohexane, L = $P(OMe)_3$: 2040 s, 2009 m, 1990 s, 1963 w, 1833 m, 1821 m	Moss, ^{13}C	Yes	8,54,89, 153
91.	$FeCo_3H(CO)_8L_4$ L = $P(OMe)_3$ L_2 = dppe	purple	cyclohexane, L = $P(OMe)_3$: 2043 w, 2022 w, 2012 m, 1985 m (br), 1945 m, 1827 w, 1816 m	Mass, Moss	No	54,89

Table I. (continued)

Index No.	Cluster[a]	Color	ν_{CO}[b]	Other Available Spectral Data[c]	Crystal Structure	Reference(s)
92.	$FeCo_3H(CO)_9(PhC_2Ph)_2$	----	----	----	No	63
93.	$[FeCo_3(CO)_{12}]^-$	purple	CH_3CN: 2066 w, 2008 s, 1974 m, 1932 m, 1815 m	----	No	39
94.	$[FeCo_3(CO)_{11}L]^-$ L = PPh_3, $PMePh_2$, $P(OPr)_3$	dark purple	THF, L = $PMePh_2$: 2007 s, 1961 vs, 1941 s, 1934 s, 1905 m (sh), 1815 vw, 1773 m (br)	^1H	No	53
95.	$[FeCo_3(CO)_{10}(dppe)]^-$	dark purple	THF: 2011 s, 1963 vs, 1944 vs, 1895 m (sh), 1807 w, 1774 m, 1749 m	^1H	No	53
96.	$[FeCo_3(CO)_{10}(PhC_2Ph)]^-$	black-violet	THF: 2043 m, 1994 s, 1980 s (sh), 1973 s (sh), 1969 s (sh), 1935 m, 1850 w, 1815 m	^1H	No	53
97.	$[Fe_2RuCo(CO)_{13}]^-$	brown	CH_2Cl_2: 2074 w, 2030 s, 2008 vs, 1997 s (sh), 1950 m (sh), 1826 w (sh), 1796 m, br	----	No	147
98.	$Fe_2Ru_2H_2(CO)_{13}$	red	2105 vw, 2084 s, 2072 m, 2066 m, 2057 s, 2041 vs, 2031 m, 2015 s, 2003 w, 1979 m, 1888 w (br), 1860 w (br)	----	No	78
99.	$Fe_2Rh_2(Cp)_2(CO)_8$	purple	2039 s, 2005 s, 1972 m, 1956 m, 1935 m, 1849 w, 1788 w	^1H	Yes	49,51,102

Table I. (continued)

Index No.	Cluster[a]	Color	ν_{CO}[b]	Other Available Spectral Data[c]	Crystal Structure	Reference(s)
100.	$Fe_2Ni_2(Cp)_2(CO)_6(RC_2R')$ R = Ph, R' = H, Ph, C_2Ph R,R' = Et		R = Ph: 2023, 1980 s, 1961	^1H	Yes	28,29,115
101.	$[Fe_3Co(CO)_{13}]^-$	black	CH_2Cl_2: 2074 w, 2004 vs, 1971 m, 1930 m (sh), 1816 m, br	----	No	40,147
102.	$Fe_3Rh(Cp)(CO)_{11}$	red	2069 s, 2033 sh, 2025 s, 1993 s, 1977 m, 1957 m, 1945 sh, 1873 m, 1826 w	^1H	Yes	50,102
103.	$[Fe_3NiH(CO)_{12}]^-$	green-brown	2060 vw, 2020 m, 1990 s, 1965 m, 1935 mw, 1875 w, 1830 w, 1790 w	^1H	No	34,40,110
104.	$[Fe_3Ni(CO)_{12}]^{2-}$	brown	THF: 2010 vw, 1955 ms, 1935 s, 1990 mw, 1810 w, 1790 w	----	No	34,40,110
105.	$[Fe_4Pd(CO)_{16}]^{2-}$	brown	THF: 1985 s, 1975 s, 1940 ms, 1920 (sh)	----	No	110,111
106.	$[Fe_4Pt(CO)_{16}]^{2-}$	green	THF: 1987 s, 1972 s, 1965 (sh), 1935 ms, 1920 (sh)	----	No	110,111
107.	$Fe_2Ir_2Cu_4(CO)_8(PPh_3)_2(C_2R)_8$ R = Ph, p-$C_6H_4CH_3$	violet	$CHCl_3$: 2048 s, 2008 s, 1982 s, 1970 s	^1H	No	2
108.	$[Fe_6Pd_6H_7(CO)_{24}]^{3-}$	----	----	----	Yes	111

Table I. (continued)

Index No.	Cluster[a]	Color	ν_{CO}[b]	Other Available Spectral Data[c]	Crystal Structure	Reference(s)
Ruthenium: (see also entries 24, 42, 45, 51, 55, 68, 69, 78-85, 97, 98)						
109.	$RuOs_2(CO)_{12}$	yellow	$CHCl_3$: 2066 vs, 2032 s, 2014 w, 2004 w	^1H	No	70,80,96
110.	$RuPt_2(CO)_5L_3$ L = PPh_3, $PMePh_2$, PMe_2Ph, $AsPh_3$, $P(OMe)_2Ph$	yellow	cyclohexane, L = PMe_2Ph: 2024 s, 1964 (sh), 1952 s, 1848 w, 1784 s	^1H	No	28,30
111.	$RuPt_2(CO)_4[P(OMe)_2Ph]_4$	yellow	cyclohexane: 1955 s, 1854 w, 1801 s, 1780 s	^1H	No	30
112.	$Ru_2Os(CO)_{12}$	yellow	$CHCl_3$: 2062 vs, 2030 s, 2013 w, 2004 w (sh)	^{13}C, Mass	No	70,80,96
113.	$Ru_2Pt(CO)_8(dppe)$	red	cyclohexane: 2073 s, 2027 s, 2001 sh, 1989 s, 1981 sh, 1972 sh, 1963 sh	^1H	No	30
114.	$Ru_2Pt(CO)_7(PMe_2Ph)_3$	yellow	cyclohexane: 2022 s, 1956 sh, 1944 s, 1853 w, 1816 s, 1768 s	^1H	No	28
115.	$RuOs_2CoH(CO)_{13}$	orange	hexane: 2122 w, 2078 s, 2056 vs, 2035 m, 2030 m, 2018 w, 1996 s, 1903 w, 1858 m	^1H	No	147
116.	$RuOs_3H_4(CO)_{12}$	yellow	2081 s, 2063 s, 2022 s, 1994 w	----	No	78

Table I. (continued)

Index No.	Cluster[a]	Color	ν_{CO}[b]	Other Available Spectral Data[c]	Crystal Structure	Reference(s)
117.	$RuCo_3H(CO)_{13}$	red	hexane: 2064 s, 2057 s, 2023 m, 2015 sh, 1887 m	Mass	No	116,161
118.	$Ru_2OsCoH(CO)_{13}$	orange	hexane: 2111 w, 2076 s, 2056 vs, 2034 m, 2028 m, 2018 m, 1907 w, 1862 m	^1H	No	147
119.	$Ru_2Os_2H_4(CO)_{12}$	yellow	2081 s, 2063 s, 2022 s, 1994 w	----	No	78
120.	$Ru_3OsH_4(CO)_{12}$	yellow	2081 s, 2063 s, 2022 s, 1994 w	----	No	78
121.	$[Ru_3Co(CO)_{13}]^-$	red	CH_2Cl_2: 2072 w, 2024 vs, 1992 m, 1823 w (sh), 1794 m, br	----	Yes	147
122.	$Ru_3CoH(CO)_{13}$	red	hexane: 2109 w, 2088 w, 2073 s, 2061 vs, 2054 vs, 2034 m, 2024 m, 2017 m, 1971 vw, 1909 w, 1865 m	^1H	No	147
123.	$Ru_3CoH_3(CO)_{12}$	red	hexane: 2111 w, 2088 s, 2080 m, 2068 s, 2052 vs, 2041 m, 2036 m, 2027 m, 2012 w, 2002 w, 1878 w (br)	^1H	Yes	81
Osmium: (see also entries 12, 13, 25, 26, 33, 34, 36, 37, 40, 41, 46-50, 52-54, 56, 70, 78, 79, 86, 109, 112, 115, 116, and 118-120)						
124.	$OsCo_2(CO)_{11}$	red	heptane: 2127 w, 2069 s, 2049 vs, 2025 m, 1823 m	----	No	121

Table I. (continued)

Index No.	Cluster[a]	Color	ν_{CO}[b]	Other Available Spectral Data[c]	Crystal Structure	Reference(s)
125.	$OsPt_2(CO)_5L_3$ L = PPh_3, $PMePh_2$	yellow	cyclohexane, L = PPh_3: 2022 s, 1943 s, 1847 w, 1795 s, 1774 s	^1H	No	28,30
126.	$Os_2Pt(CO)_7(PMe_2Ph)_3$	orange	cyclohexane: 2018 s, 1944 m, 1848 w, 1820 m, 1756 m	^1H	No	28,30
127.	$OsCo_3H(CO)_{12}$	red	hexane: 2064 s, 2056 s, 2018 m, 1890 m, 1109 (KBr)	Mass	No	103
128.	$Os_2Co_2H_2(CO)_{12}$	orange	hexane: 2112 w, 2081 s, 2078 s, 2057 vs, 2046 s, 2028 m, 2015 m	----	No	121
129.	$Os_2Pt_2H_2(CO)_8(PPh_3)_2$	----	cyclohexane: 2059 s, 2031 vs, 2011 w, 1981 s, 1963 w, 1943 m	^1H, ^{31}P	Yes	30,67
130.	$Os_3CoH_3(CO)_{12}$	pale yellow	cyclohexane: 2076 vs, 2066 ms, 2049 w, 2030 vs, 2025 vs, 2012 w, 2005 s, 2000 sh, 1982 w	^1H, ^{13}C	Yes	23
131.	$Os_3RhH_2(CO)_{10}(acac)$	black	----	^1H	No	67
132.	$Os_3NiH_2(CO)_{10}(PPh_3)_2$	orange	2073 s, 2065 m, 2037 vs, 2015 s, 1999 s, 1985 m (sh), 1973 m, 1959 w (sh), 1855 m, 1821 m	^1H, ^{31}P	No	67

Table I. (continued)

Index No.	Cluster[a]	Color	ν_{CO}[b]	Other Available Spectral Data[c]	Crystal Structure	Reference(s)
133.	$Os_3PtH_2(CO)_{10}(PPh_3)L$ L = PPh_3, $AsPh_3$	----	----	^1H, ^{31}P	No	67
134.	$Os_3PtH_2(CO)_{11}(PPh_3)$	----	----	^{31}P	No	67
135.	$Os_3PtH_2(CO)_{10}L$ L = PPh_3, PCy_3	dark green	cyclohexane, L = PPh_3: 2079 m, 2053 sh, 2045 s, 2029 vw, 2019 s, 1989 s, 1975 m, 1963 w, 1947 w	^1H	Yes	67
136.	$Os_3AuX(CO)_{10}L$ L = PPh_3, X = Cl, Br, I, SCN L = $P(C_6H_4Me)_3$, X = Cl	red	cyclohexane, L = PPh_3, X = Cl: 2096 m, 2045 vs, 2016 s, 2009 s, 1990 sh, 1983 m, 1976 w (sh), 1965 m	Raman, Mass	Yes	24
137.	$Os_3AuH(CO)_{10}(PPh_3)$	green	----	^1H	No	67
138.	$Os_3Au_2(CO)_{10}(PPh_3)_2S_2$	orange	cyclohexane: 2060 m, 2032 s, 2020 s, 1988 sh, 1973 m, 1955 s	----	No	24
Cobalt: (see also entries 1-3, 8, 14, 27, 57-63, 71, 72, 80, 87-97, 101, 115, 117, 118, 121-124, 127, 128, and 130)						
139.	$CoNi_2(Cp)_3(CO)_2$	----	1723	----	Yes	157
140.	$Co_2Pt(CO)_7L_2$ L_2 = dppe, dpae	red-brown	KBr: 2049 s, 2010 s 1975 vs, 1970 sh, 1729 s	----	No	59

Table I. (continued)

Index No.	Cluster[a]	Color	ν_{CO}[b]	Other Available Spectral Data[c]	Crystal Structure	Reference(s)
141.	$Co_2Rh_2(CO)_{12}$	brown	pentane: 2074 w, 2064 s, 2059 s, 2038 m, 2030 m, 1920 w, 1910 sh, 1885 s, 1871 s, 1855 w	UV	No	113
142.	$Co_2Rh_2(CO)_{10}(PF_3)_2$	deep brown	pentane: 2104 vw, 2096 s, 2078 sh, 2070 vs, 2062 sh, 2047 s, 1924 w, 1889 s, 1878 s, 1863 sh	^{19}F, ^{31}P	No	65
143.	$Co_2Rh_2(CO)_8(PF_3)_4$	deep brown	pentane: 2094 s, 2086 w (sh), 2070 vs, 2062 vw (sh), 2045 s, 2035 vw (sh), 1922 m, 1887 s, 1874 s	^{31}P, ^{19}F	No	65
144.	$Co_2Ir_2(CO)_{12}$	dark red	pentane: 2072 s, 2061 s, 2055 s, 2036 m, 2033 m, 2030 m, 1885 w,	UV, Mass	Yes	14,113
145.	$Co_2Ir_2(CO)_8(PF_3)_4$	dark brown	pentane: 2090 w (sh), 2075 s (sh), 2068 s, 2044 m, 2035 (sh), 2018 m, 1872 s (br), 1865 s (br)	----	No	65
146.	$Co_2Pt_2(CO)_8L_2$ L = PPh_3, PEt_3	red	toluene, L = PPh_3: 2061 s, 2034 vs, 2018 sh, 1992 s, 1937 m, 1871 m, 1825 s, 1820 s	----	Yes	20,26,71

Table I. (continued)

Index No.	Cluster[a]	Color	ν_{CO}[b]	Other Available Spectral Data[c]	Crystal Structure	Reference(s)
141.	$Co_2Rh_2(CO)_{12}$	brown	pentane: 2074 w, 2064 s, 2059 s, 2038 m, 2030 m, 1920 w, 1910 sh, 1885 s, 1871 s, 1855 w	UV	No	113
142.	$Co_2Rh_2(CO)_{10}(PF_3)_2$	deep brown	pentane: 2104 vw, 2096 s, 2078 sh, 2070 vs, 2062 sh, 2047 s, 1924 w, 1889 s, 1878 s, 1863 sh	^{19}F, ^{31}P	No	65
143.	$Co_2Rh_2(CO)_8(PF_3)_4$	deep brown	pentane: 2094 s, 2086 w (sh), 2070 vs, 2062 vw (sh), 2045 s, 2035 vw (sh), 1922 m, 1887 s, 1874 s	^{31}P, ^{19}F	No	65
144.	$Co_2Ir_2(CO)_{12}$	dark red	pentane: 2072 s, 2061 s, 2055 s, 2036 m, 2033 m, 2030 m, 1885 w,	UV, Mass	Yes	14,113
145.	$Co_2Ir_2(CO)_8(PF_3)_4$	dark brown	pentane: 2090 w (sh), 2075 s (sh), 2068 s, 2044 m, 2035 (sh), 2018 m, 1872 s (br), 1865 s (br)	----	No	65
146.	$Co_2Pt_2(CO)_8L_2$ L = PPh_3, PEt_3	red	toluene, L = PPh_3: 2061 s, 2034 vs, 2018 sh, 1992 s, 1937 m, 1871 m, 1825 s, 1820 s	----	Yes	20,26,71

Table I. (continued)

Index No.	Cluster[a]	Color	ν_{CO}[b]	Other Available Spectral Data[c]	Crystal Structure	Reference(s)
147.	$Co_3Rh(CO)_{12}$	brown	pentane: 2066 m, 2059 s, 2056 sh, 2037 m, 2031 m, 1909 w, 1882 s, 1856 s	UV, Mass, ^{13}C	No	113
148.	$[Co_3Ni(CO)_{11}]^-$	brown	THF: 2050 vw, 2000 vs, 1960 m, 1950 sh, 1865 m, 1845 m, 1740 m	----	No	38
149.	$Co_3Ni(Cp)(CO)_8(CNR)$ R = Me, t-Bu	----	hexane, R = Me: 2057 m, 2029 w, 2013 s, 2006 s, 1845 m, 1838 m, 1830 sh	----	No	126
150.	$Co_3Ni(Cp)(CO)_9$	green	hexane: 2082 s, 2043 vs, 2025 vs, 1850 s	^1H	No	87
151.	$Co_2Pt_3(CO)_9(PEt_3)_3$	dark violet	2016 s, 1998 sh, 1980 s, 1848 w, 1860 w, 1825 s, 1807 s, 1761 m	----	Yes	20
152.	$Co_2Rh_4(CO)_{16}$	----	----	----	No	113,150
153.	$[Co_2Rh_4(CO)_{15}C]^{2-}$	----	----	----	No	10
154.	$[Co_4Ni_2(CO)_{14}]^{2-}$	dark red	THF: 2020 w, 1990 sh, 1977 s, 1958 s, 1790 m, 1749 sh	----	Yes	13,38

Table I. (continued)

Index No.	Cluster[a]	Color	ν_{CO}[b]	Other Available Spectral Data[c]	Crystal Structure	Reference(s)
Rhodium: (see also entries 64, 73, 99, 102, 131, 141-143, 147, 152 and 153)						
155.	$Rh_2Ir_2(CO)_{12}$	orange	pentane: 2071 s, 2042 m, 2034 m, 2022 w, 1923 w, 1887 s, 1867 s, 1855 w	UV, Mass	No	113
	$Rh_2Cu_4(PPh_2R)_2(C_2Ar)_8$ R = Me, Ph; Ar = Ph, p-C_6H_4Me, p-C_6H_4F	violet	----	IR, ^1H	No	2
157.	$Rh_3Ir(CO)_{12}$	orange	heptane: 2073 m, 2070 s, 2042 s, 2034 w, 2021 m, 1887 s	UV, Mass	No	113
158.	$[Rh_4Pt(CO)_{14}]^{2-}$	yellow-brown	THF: 2000 s, 1956 s, 1810 m, 1790 m, 1735 w	^{195}Pt	Yes	34,75
159.	$[Rh_5Pt(CO)_{15}]^-$	brown	THF: 2082 vw, 2038 s, 2011 m, 1791 ms	^{195}Pt	Yes	75
Iridium: (see also entries 107, 144, 145, 155, and 157)						
160.	$IrCu_3(PPh_3)_3(C_2Ph)_2$	buff	----	IR	No	2
161.	$Ir_2Cu_4(PPh_2R)_2(C_2Ar)_8$ R = Me; Ar = Ph, C_6H_5 R = Ph; Ar = Ph, p-C_6H_4Me, p-C_6H_4F	purple	----	^1H	Yes	2,3,45
Nickel: (see entries 9, 16, 19, 21, 29, 35, 65, 66, 74, 75, 100, 103, 104, 132, 139, 148-150, and 154)						
Palladium: (see entries 17, 22, 105, and 108)						

Table I. (continued)

Platinum: (see entries 6, 11, 18, 20, 23, 43, 67, 76, 77, 106, 110, 111, 113, 114, 125, 126, 129, 133-135, 140, 146, 151, 158, and 159)

Copper: (see entries 107, 156, 160 and 161)

Gold: (see entries 44, and 136-138)

---

[a] Cp = η^5-C_5H_5; dppe = $Ph_2PCH_2CH_2PPh_2$; diars = o-$(AsPh_2)_2C_6H_4$; acac = $CH_3C(O)CHC(O)CH_3$; dpae = $Ph_2AsCH_2CH_2AsPh_2$; Ph = C_6H_5; Bu = C_4H_9; Cy = C_6H_{11}; Me = CH_3; Et = C_2H_5; Pr = C_3H_7.

[b] THF = tetrahydrofuran.

[c] Mass = mass spectral data; Moss = Mossbauer data; IR = infrared data other than ν_{CO}; UV-VIS = electronic absorption spectral data; ^1H = ^1H NMR data; ^{31}P = ^{31}P NMR data; ^{13}C = ^{13}C NMR data; ^{19}F = ^{19}F NMR data; ^{195}Pt = ^{195}Pt NMR data; Raman = Raman spectral data.

Table II. Effect of Ligand Size and Basicity on the $C_1 \rightleftarrows C_s$ Equilibrium of $FeRu_3H_2(CO)_{11}L$ (82)

Ligand	Cone Angle (degrees)[a]	Basicity (cm^{-1})[a]	K
$P(i\text{-}Pr)_3$	160	2059.2	>100
PPh_3	145	2068.9	>100
$PMePh_2$	136	2067.0	11
PEt_2Ph	136	2063.7	11
$P(OMe)_3$	107	2079.5	10
$P(OEt)_2Ph$	116	2074.2	5.5
PMe_2Ph	122	2065.3	1.8
PMe_3	118	2064.1	0.4

[a]Data taken from Tolman, C. A., Chem. Rev., 77, 313 (1977).

References

1. Abu Salah, O. M., and Bruce, M. I., J. Chem. Soc. Dalton Trans., 2311 (1975).

2. Abu Salah, O. M., and Bruce, M. I., Aust. J. Chem., 29, 531 (1976).

3. Abu Salah, O. M., Bruce, M. I., Beznan, S. A., and Churchill, M. R., J. Chem. Soc. Chem. Commun., 858 (1972).

4. Abu Salah, O. M., Bruce, M. I., Churchill, M. R., and DeBoer, B. G., J. Chem. Soc. Chem. Commun. 688 (1974).

5. Agapiou, A., Jordan, R. F., Zyzyck, L. A., and Norton, J. A., J. Organomet. Chem., 141, 35 (1977).

6. Agapiou, A., Pedersen, S. E., Zyzyck, L. A. and Norton, J. R., J. Chem. Soc. Chem Commun., 393 (1977).

7. Aime, S., and Milone, L., Prog. NMR Spectra, 11, 183 (1977).

8. Aime, S., Milone, L., Osella, D., and Poli, A., Inorg. Chim. Acta., 30, 45 (1978).

9. Aime, S., Milone, L., Rossetti, R. and Stanghellini, P. L., Inorg. Chim. Acta., 25, 103 (1977).

10. Albano, V. G., Chini, P., Martinengo, S., Sansoni, M., and Strumolo, D., J. Chem. Soc. Chem. Commun., 299 (1974).

11. Albano, V. G., and Ciani, G., J. Organomet. Chem., 66, 311 (1974).

12. Albano, V. G., Ciani, G., Bruce, M. I., Shaw, G., and Stone, F. G. A., J. Organomet. Chem., 42, C99 (1972).

13. Albano, V. G., Ciani, G., and Chini, P., J. Chem. Soc. Dalton Trans., 432 (1974).

14. Albano, V. G., Ciani, G., and Martinengo, S., J. Organomet. Chem., 78, 265 (1974).

15. Anders, U. and Graham, W. A. G., J. Chem. Soc., Chem. Commun., 291 (1966).

16. Anders, A., and Graham, W. A. G., J. Am. Chem. Soc., 89, 539 (1967).

17. Anderson, J. R., Elmes, P. S., Horne, R. F., and Mainwaring, D. E., J. Catal., 50, 508 (1977).

18. Ashworth, T. V., Berry, M., Howard, J. A. K., Laguna, M. and Stone, F. G. A., J. Chem. Soc. Chem. Commun., submitted for publication.

19. Ashworth, T. V., Howard, J. A. K., and Stone, F. G. A., J. Chem. Soc. Chem., Commun., submitted for publication.

20. Barbier, J. P., Braunstein, P., Fischer, J., and Ricard, L., Inorg. Chim. Acta, 31, L361 (1978).

21. Bender, R., Braunstein, P., Dusausoy, Y., and Protas, J., Angew. Chem. Int. Ed. Engl., 17, 596 (1978).

22. Bennett, M. J., Graham, W. A. G., Hoyano, J. K., and Hutcheon, W. L., J. Am. Chem. Soc., 94, 6232 (1972).

23. Bhoduri, S., Johnson, B. F. G., Lewis, J., Raithby, P. R., and Watson, D. J., J. Chem. Soc. Chem. Commun., 343 (1978).

24. Bradford, C. W., van Bronswijk, W., Clark, R. J. H., and Nyholm, R. S., J. Chem. Soc. A, 2889 (1970).

25. Braunstein, P. and Dehand, J., Bull. Soc. Chim. Fr., 1997 (1975).

26. Braunstein, P., Dehand, J., and Nennig, J. F., J. Organomet. Chem., 92, 117 (1975).

27. Bruce, M. I., Abu Salah, O. M., Davis, R. E., and Raghovan, N. V., J. Organomet. Chem., 64, C48 (1974).

28. Bruce, M. I., Shaw, G., and Stone, F. G. A., J. Chem. Soc. Chem Commun., 1288 (1971).

29. Bruce, M. I., Shaw, G., and Stone, F. G. A., J. Chem. Soc. Dalton Trans., 1082 (1972).

30. Bruce, M. I., Shaw, G. and Stone, F. G. A., J. Chem. Soc. Dalton Trans., 1781 (1972).

31. Burger, K., Korecz, L., and Bor, G., J. Inorg. Nucl. Chem., 31, 1527 (1969).

32. Burt, J. C. and Schmid, G., J. Chem. Soc. Dalton Trans., 1385 (1978).

33. Catton, G. A., Jones, G. F. C., Mays, M. J., and Howell, J. A. S., Inorg. Chim. Acta., 20, L41 (1976).

34. Chini, P., private communication, 1978.

35. Chini, P., XVII Int. Cong. Pure Appl. Chem., Munich, August 30 - Sept. 6, 1959.

36. Chini, P., Inorg. Chim. Acta. Rev., 2, 31 (1968).

37. Chini, P., Pure Appl. Chem., 23, 489 (1970).

38. Chini, P., Cavalieri,A., and Martinengo, S., Coord. Chem. Rev., 8, 3 (1972).

39. Chini, P., Colli, L., and Peraldo, M., Gazz. Chim. Ital., 90, 1005 (1960).

40. Chini, P., and Heaton, B. T., Topics Curr. Chem., 71, 1 (1977).

41. Chini, P., Longoni, G., and Albano, V. G., Adv. Organomet. Chem., 14, 285 (1976).

42. Chini, P., Martinengo, S., and Longoni, G., Gazz.Chim. Ital., 105, 203 (1975).

43. Christian, P. A., Ph.D. Thesis, Stanford University, 1978.

44. Churchill, M. R., and Bau, R., Inorg. Chem., 6, 2086 (1967).

45. Churchill, M. R. and Beznan, S. A., Inorg. Chem., 13, 1418 (1974).

46. Churchill, M. R., and DeBoer, B. G., Inorg.Chem., 14, 2630 (1975).

47. Churchill, M. R., and Hollander, F. J., Inorg. Chem., 16, 2493 (1977).

48. Churchill, M. R., Hollander, F. J., Shapley, J. R., and Foose, D. S., J. Chem. Soc., Chem. Commun., 534 (1978).

49. Churchill, M. R., and Veidis, M. V., J. Chem. Soc. Chem. Commun., 529 (1970).

50. Churchill, M. R. and Veidis, M. V., J. Chem. Soc. Chem. Commun., 1470 (1970).

51. Churchill, M. R. and Veidis, M. V., J. Chem. Soc. A, 2170 (1971).

52. Collman, J. P., Finke, R. G., Matlock, P. L., Wahren, R., Komoto, R. G., and Brauman, J. F., J. Am. Chem. Soc., 100, 1119 (1978).

53. Cooke, C. G., and Mays, M. J., J. Organomet. Chem., 74, 449 (1974).

54. Cooke, C. G., and Mays, M. J., J. Chem. Soc. Dalton Trans., 455 (1975).

55. Cotton, F. A., Q. Rev., Chem. Soc., 20, 389 (1966).

56. Cotton, F. A., Kruczymsk, L., Shapiro, B. L., and Johnson, L. T., J. Am. Chem. Soc., 94, 6191 (1972).

57. Curtis, M. D., and Klinger, R. J., J. Organomet. Chem., 161, 23 (1978).

58. Dahl, L. F. and Smith, D. L., J. Am. Chem. Soc., 84, 2450 (1962).

59. Dehand, J., and Nennig, J. F., Inorg. Nucl. Chem. Lett., 10, 875 (1974).

60. Dehand, J. and Pfeffer, M., J. Organomet. Chem., 104, 377 (1976).

61. Ehrl, W. and Vahrenkamp, Chem. Ber., 106, 2556 (1973); 106, 2563 (1973).

62. Enos, C. T., Geoffroy, G. L., and Risby, T. H., J. Chromatogr. Sci., 15, 83 (1977).

63. Epstein, R. and Geoffroy, G. L., unpublished observations.

64. Epstein, R. A., Withers, H. W., and Geoffroy, G. L., Inorg. Chem. in press (1979).

65. Eshtiagh-Hosseini, H., and Nixon, J. F., J. Organomet. Chem., 150, 129 (1978).

66. Evans, G. O., Hargaden, J. P., and Sheline, R. K., J. Chem. Soc., Chem. Commun., 186 (1967).

67. Farrugia, L. J., Howard, J. A. K., Mitrprachachon, P., Spencer, J. L., Stone, F. G. A., and Woodward, P., J. Chem. Soc. Chem. Commun., 260 (1978).

68. Farrugia, L. J., Howard, J. A. K., Mitrprachachon, P., Spencer, J. L., Stone, F. G. A., and Woodward, P., to be published (1979).

69. Fellmann, W., and Kaesz, H. D., Inorg. Nucl. Chem. Lett., 2, 63 (1966).

70. Ferrari, R. P., Vaglio, G. A., and Valle, M., J. Chem. Soc. Dalton Trans., 1164 (1978).

71. Fischer, J., Mitschler, A., Weiss, R., Dehand, J., and Nennig, J. F., J. Organomet. Chem., 91, C37 (1975).

72. Ford, P. C., Rinker, R. G., Ungermann, C., Laine, R. M., Landis, V., and Moya, S. A., J. Am. Chem. Soc., 100, 4595 (1978).

73. Forster, A., Johnson, B. F. G., Lewis, J., Matheson, T. W., Robinson, B. H. and Jackson, W. G., J. Chem. Soc. Chem. Commun., 1042 (1974).

74. Fox, J. R., Gladfelter, W. L., Geoffroy, G. L., Day, V. W., Abdel-Meguid, S., and Tavanailpour, I., J. Am. Chem. Soc., to be submitted.

75. Fumagalli, A., Martinengo, S., Chini, P., Albinati, A., Bruckner, S., and Heaton, B. T., J. Chem. Soc. Chem. Commun., 195 (1978).

76. Geoffroy, G. L. and Epstein, R. A., Inorg. Chem., 16, 2795 (1977).

77. Geoffroy, G. L., and Gladfelter, W. L., J. Am. Chem. Soc., 99, 6775 (1977).

78. Geoffroy, G. L., and Gladfelter, W. L., J. Am. Chem. Soc., 99, 7565 (1977).

79. Gilmore, C. J. and Woodward, P., J. Chem. Soc. A, 3453 (1971).

80. Gladfelter, W. L., Fox, J. R. and Geoffroy, G. L., unpublished results.

81. Gladfelter, W. L., Geoffroy, G. L., and Calabrese, J., Inorg. Chem., to be submitted (1979).

82. Gladfelter, W. L., Smegal, J. A., Foreman, T. A., and Geoffroy, G. L., J. Organomet. Chem. submitted for publication.

83. Haines, R. J., Burckett-St. Laurent, J. C., and Nolte, C. R., J. Organomet. Chem., 104, C27 (1976).

84. Haines, R. J., Mason, R., Zubieta, J. A., and Nolte, C. R., J. Chem. Soc. Chem. Commun., 990 (1972).

85. Haustein, H. J. and Schwarzhans, K. E., Z. Naturforsch., 33B, 1108 (1978).

86. Howell, J. A. S., Matheson, T. W., and Mays, M. J., J. Organomet. Chem., 88, 363 (1975).

87. Hsieh, A. T. T. and Knight, J., J. Organomet. Chem., 26, 125 (1971).

88. Hsieh, A. T. T., and Mays, M. J., J. Organomet. Chem., 39, 157 (1972).

89. Huie, B. T., Knobler, C. B., and Kaesz, H. D., J. Am. Chem. Soc., 100, 3059 (1978).

90. Humphries, A. P., and Kaesz, H. D., Prog. Inorg. Chem., in press.

91. Huttner, G., Frank, A., and Mohr, G., Z. Naturforsch., 31b, 1161 (1976).

92. Hutter, G., Mohr, G., and Frank, A., Angew. Chem., Int. Ed. Engl., 15, 682 (1976).

93. Huttner, G., Mohr, G., and Friedrick, P., Z. Naturforsch., 33B, 1254 (1978).

94. Inkrott, K. E. and Shore, S. G., J. Am. Chem. Soc., 100, 3954 (1978).

95. Jackman, L. M. and Cotton, F. A., Ed., "Dynamic Nuclear Magnetic Resonance Spectroscopy", Academic Press, New York, N.Y. 1975.

96. Johnson, B. F. G., Johnston, R. D., Lewis, J., Williams, I. G., and Kilty, P. A., J. Chem. Soc., Chem. Commun., 861 (1968).

97. Johnson, B. F. G., Lewis, J., and Matheson, T. W., J. Chem. Soc., Chem. Commun., 441 (1974).

98. Johnson, B. F. G., Lewis, J., Reichert, B., Schorpp, K. T., and Sheldrick, G. M., J. Chem. Soc. Dalton Trans., 1417 (1977).

99. Khattab, S. A., Marko, L., Bor, G., and Marko, B., J. Organomet. Chem., 1, 373 (1964).

100. King, R. B., Prog. Inorg. Chem., 15, 287 (1972).

101. Knight, J. and Mays, M. J. Chem. Ind. London, 1159 (1968).

102. Knight, J. and Mays, M. J., J. Chem. Soc. A, 654 (1970).

103. Knight, J. and Mays, M. J., J. Chem. Soc. A, 711 (1970).

104. Knight, J. and Mays, M. J., J. Chem. Soc. Chem. Commun., 1006 (1970).

105. Knight, J., and Mays, M. J., J. Chem. Soc. Chem. Commun., 62 (1971).

106. Knight, J. and Mays, M. J., J. Chem. Soc., Dalton Trans., 1022 (1972).

107. Knox, S. A. R., Koepke, J. W., Andrews, M. A., and Kaesz, H. D., J. Am. Chem. Soc., 97, 3942 (1975).

108. Labroue, D. and Poilblanc, R., J. Mol. Catal., 2, 329 (1977).

109. Lindauer, M. W., Evans, G. O., and Sheline, R. K., Inorg. Chem., 7, 1249 (1968).

110. Longoni, G. and Manassero, M., 3rd European Inorg. Chem. Sym., Cortova, Italy, April 24-28, 1978.

111. Longoni, G. and Manassero, M., unpublished results (communicated by P. Chini).

112. Martinengo, S. and Chini, P., Gazz. Chim. Ital., 102, 344 (1972).

113. Martinengo, S., Chini, P., Albano, V. G., Cariati, F. and Salvatori, T., J. Organomet. Chem., 59, 379 (1973).

114. Mason, R. and Zubieta, J. A., J. Organomet. Chem., 66, 279 (1974).

115. Mason, R., Zubieta, J., Hsieh, A. T. T., Knight, J., and Mays, M. J., J. Chem. Soc. Chem. Commun., 200 (1972).

116. Mays, M. J., and Simpson, R. N. F., J. Chem. Soc. A, 1444 (1968).

117. Meyer, J. L. and McCarley, R. E., Inorg. Chem., 17, 1867 (1978).

118. Milone, L., private communication, 1978.

119. Milone, L., Aime, S., Randall, E. W., and Rosenberg, E., J. Chem. Soc. Chem. Commun., 452 (1975).

120. Modinos, A., and Woodward, P., J. Chem. Soc. Dalton Trans., 1534 (1975).

121. Moss, J. R. and Graham, W. A. G., J. Organomet. Chem. 23, C23 (1970).

122. Moss, J. R., and Graham, W. A. G., Inorg. Chem., 76, 75 (1977).

123. Muetterties, E. L., Bull. Soc. Chim. Belg., 84, 959 (1975).

124. Muetterties, E. L., Science, 196, 839 (1977).

125. Muetterties, E. L., Rhodin, T. N., Band, E., Brucker, C. F., and Pretzer, W. R., in press.

126. Newman, J. and Manning, A. R., J. Chem. Soc. Dalton Trans., 2549 (1974).

127. Ozin, G. A., Catal. Rev.-Sci. Eng., 16, 191 (1977).

128. Pearson, R. G. and Dehand, J., J. Organomet. Chem., 16, 485 (1969).

129. Pittman, C. U., Jr., and Ryan, R. C., Chemtech, 170 (1978).

130. Raverdino, V., Aime, S., Milone, L., and Sappa, E., Inorg. Chim. Acta, 30, 9 (1978).

131. Renaut, P., Tainturier, G., and Gautheron, B., J. Organomet. Chem., 150, C9 (1978).

132. Richter, F., and Vahrenkamp, H., Angew. Chem. Int. Ed. Engl., 17, 444 (1978).

133. Rossetti, R., Gervasio, G., and Stanghellini, P. L., J. Chem. Soc., Dalton Trans., 222 (1978).

134. Ruff, J. K., White, R. P., Jr., and Dahl, L. F., J. Am. Chem. Soc., 93, 2159 (1971).

135. Schafer, H. and Spreckelmeyer, B., J. Less.-Common Met., 11, 73 (1966).

136. Schmid, G., Angew. Chem. Int. Ed. Engl., 17, 392 (1978).

137. Schmid, G., Bartl, K., and Boese, R., Z. Naturforsch., 32b, 1277 (1977).

138. Schmid, G., Batzel, V., Stutte, B., J. Organomet. Chem., 113, 67 (1976).

139. Schmid, G., Stutte, B., Boese, R., Chem. Ber., 111, 1239 (1978).

140. Schwarzhans, K. E. and Steiger, H., Angew. Chem. Int. Ed. Engl., 11, 535 (1972).

141. Shapley, J. R., Strem. Chemiker, 6, 3 (1978).

142. Shapley, J. R., private communication, 1978.

The compound originally formulated as $HReOs_3(CO)_{15}$ in ref 143 was shown to be $HReOs_3(CO)_{15}(CH_3CN)$.

143. Shapley, J. R., Pearson, G. A., and Foose, D. S., 175th National Meeting of the American Chemical Society, Anaheim, Ca., March 12-17, 1978. Abstr Inorg. 74.

144. Shapley, J. R., Pearson, G. A., Tachikawa, M., Schmidt, G., Churchill, M. R., and Hollander, F. J., J. Am. Chem. Soc. 99, 8064 (1977).

145. Smith, A. K., and Basset, J. M., J. Mol. Catal., 2, 229 (1977).

146. Soltmann, B., Smeeley, C. C., and Holland, J. F., Analyt. Chem., 49, 1164 (1977).

147. Steinhardt, P. C., Gladfelter, W. L., and Geoffroy, G. L., to be submitted, 1979.

148. Stevenson, D. L., Wei, C. H., and Dahl, L. F., J. Am. Chem. Soc., 93, 6027 (1971).

149. Stone, F. G. A., private communication, 1978.

132. Richter, F., and Vahrenkamp, H., Angew. Chem. Int. Ed. Engl., 17, 444 (1978).

133. Rossetti, R., Gervasio, G., and Stanghellini, P. L., J. Chem. Soc., Dalton Trans., 222 (1978).

134. Ruff, J. K., White, R. P., Jr., and Dahl, L. F., J. Am. Chem. Soc., 93, 2159 (1971).

135. Schafer, H. and Spreckelmeyer, B., J. Less.-Common Met., 11, 73 (1966).

136. Schmid, G., Angew. Chem. Int. Ed. Engl., 17, 392 (1978).

137. Schmid, G., Bartl, K., and Boese, R., Z. Naturforsch., 32b, 1277 (1977).

138. Schmid, G., Batzel, V., Stutte, B., J. Organomet. Chem., 113, 67 (1976).

139. Schmid, G., Stutte, B., Boese, R., Chem. Ber., 111, 1239 (1978).

140. Schwarzhans, K. E. and Steiger, H., Angew. Chem. Int. Ed. Engl., 11, 535 (1972).

141. Shapley, J. R., Strem. Chemiker, 6, 3 (1978).

142. Shapley, J. R., private communication, 1978.

The compound originally formulated as $HReOs_3(CO)_{15}$ in ref 143 was shown to be $HReOs_3(CO)_{15}(CH_3CN)$.

143. Shapley, J. R., Pearson, G. A., and Foose, D. S., 175th National Meeting of the American Chemical Society, Anaheim, Ca., March 12-17, 1978. Abstr Inorg. 74.

144. Shapley, J. R., Pearson, G. A., Tachikawa, M., Schmidt, G., Churchill, M. R., and Hollander, F. J., J. Am. Chem. Soc. 99, 8064 (1977).

145. Smith, A. K., and Basset, J. M., J. Mol. Catal., 2, 229 (1977).

146. Soltmann, B., Smeeley, C. C., and Holland, J. F., Analyt. Chem., 49, 1164 (1977).

147. Steinhardt, P. C., Gladfelter, W. L., and Geoffroy, G. L., to be submitted, 1979.

148. Stevenson, D. L., Wei, C. H., and Dahl, L. F., J. Am. Chem. Soc., 93, 6027 (1971).

149. Stone, F. G. A., private communication, 1978.

150. Stone, F. G. A., and Chaston, S. H. H., 11th Int. Coord. Chem. Conf., Haifa, Israel, Sept. 8-12, 1968.

151. Strouse, C. E., and Dahl, L. F., J. Am. Chem. Soc. 93, 6032 (1971).

152. Stutte, B., Batzel, V., Boese, R., Schmid, G., Chem. Ber. 111, 1603 (1978).

153. Teller, R. G., Wilson, R. D., McMullan, R. K., Koetzel, T., and Bau, R., J. Am. Chem. Soc., 100, 3071 (1978).

154. Teo, B. K., Ph.D. Thesis, University of Wisconsin, Madison, Wis., 1974.

155. Tilney-Bassett, J. F., J. Chem. Soc., 4784 (1963).

156. Tyler, D. R., Levenson, R. A., and Gray, H. B., J. Am. Chem. Soc., 100, 7888 (1978).

157. Uchtman, V. A., and Dahl, L. F., J. Am. Chem. Soc., 91, 3763 (1969).

158. Vergamini, P. J., Vahrenkamp, H., and Dahl, L. F., J. Am. Chem. Soc., 93, 6326 (1971).

159. Wade, K., Adv. Inorg. Chem. Radiochem., 18, 1 (1976).

160. Wender, I and Pino, P., "Organic Synthesis via Metal Carbonyls", Vol. 1, Wiley-Interscience, New York, N.Y., 1968.

161. Yawney, D. B. W., and Stone, F. G. A., J. Chem. Soc. A, 502 (1969).

Figure Captions

Figure 1. Low resolution electron-impact mass spectrum of $H_2FeRu_2OsH_2(CO)_{13}$.

Figure 2. Comparison of observed (——) and calculated (----) isotopic distribution of the parent ion of $FeRuOs_2H_2(CO)_{13}$.

Figure 3. Carbonyl region infrared spectra of a) $FeRu_3H_2(CO)_{13}$, b) $FeRu_2OsH_2(CO)_{13}$, c) $FeRuOs_2H_2(CO)_{13}$, and d) $FeOs_3H_2(CO)_{13}$ measured in cyclohexane solution.

Figure 4. Electronic absorption spectra of $FeRu_3H_2(CO)_{13}$ (——), $FeRu_2OsH_2(CO)_{13}$ (----), and $FeRuOs_2H_2(CO)_{13}$ (••••) measured in hexane solution.

Figure 5. High pressure liquid chromatogram of the mixture of clusters obtained from the addition of $[Co(CO)_4]^-$ to $Ru_3(CO)_{12}$, followed by protonation with H_3PO_4. The separation was achieved using a 25-cm Waters Associates μ-Porasil column with hexane as the eluting solvent at a flow rate of 1.5 ml/min.

Figure 6. $^{13}C\{^1H\}$ NMR spectrum of $FeRuOs_2H_2(CO)_{13}$ at -60°C.

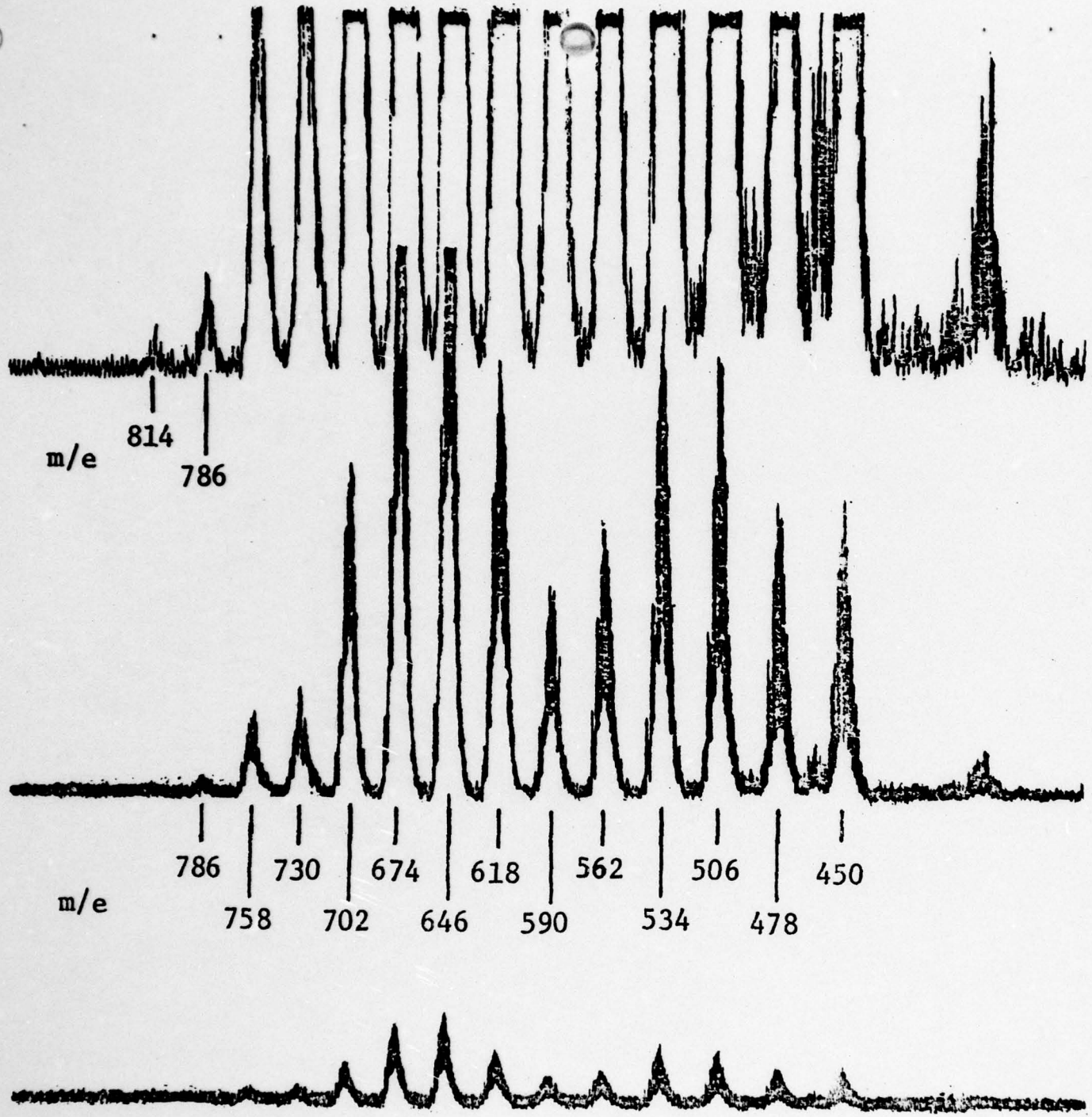
814
786
m/e
786
730
674
618
562
506
450
758
702
646
590
534
478
m/e

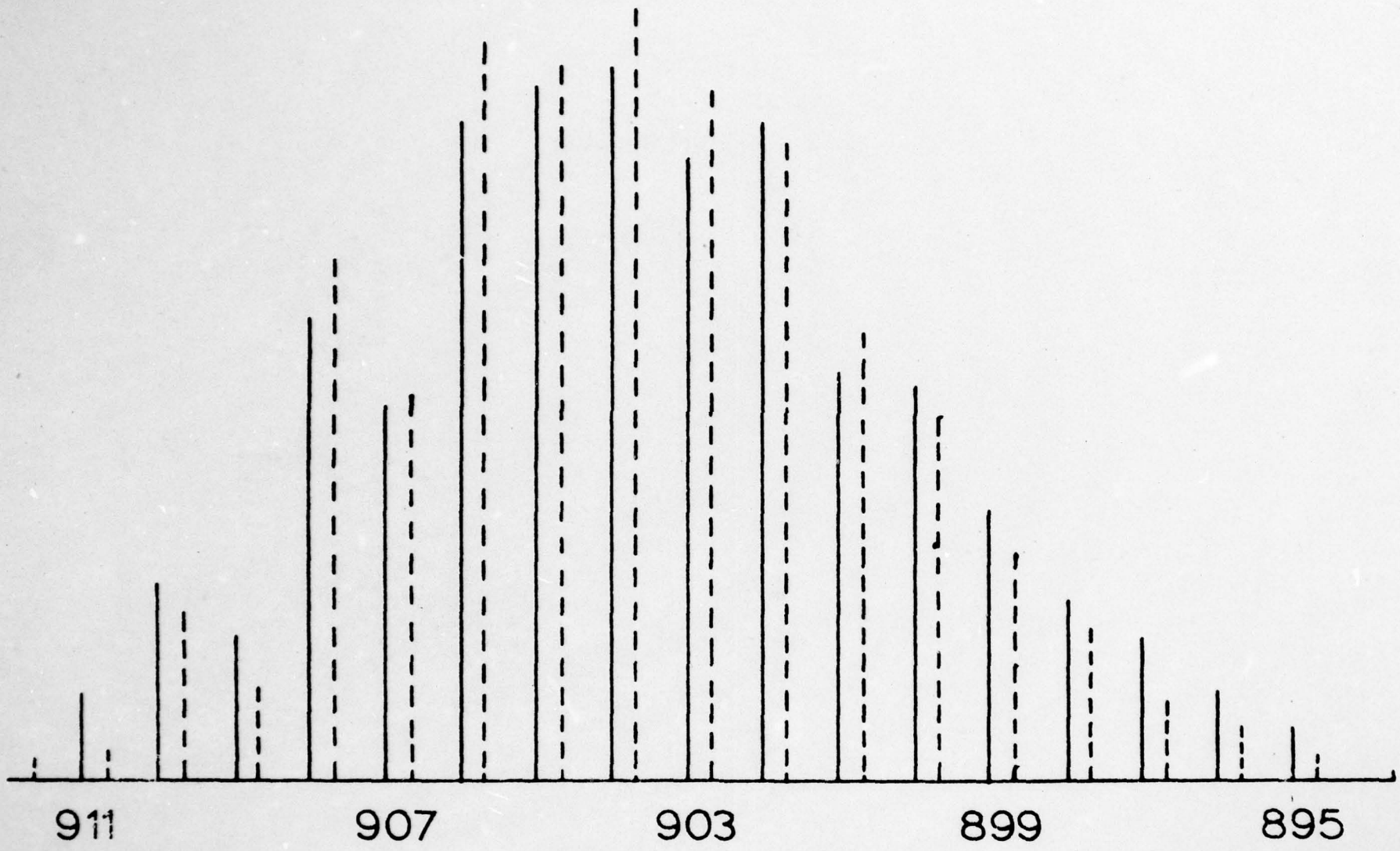
911
907
903
899
895

AD-A065 108 PENNSYLVANIA STATE UNIV UNIVERSITY PARK DEPT OF CHEMISTRY F/G 7/2
MIXED-METAL CLUSTERS.(U)
FEB 79 W L GLADFELTER, G L GEOFFROY N00014-77-C-0417
UNCLASSIFIED TR-79-1 NL

2 OF 2
AD
A065108

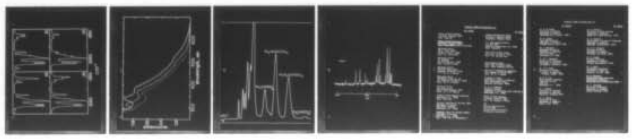

END
DATE
FILMED
4 -79
DDC

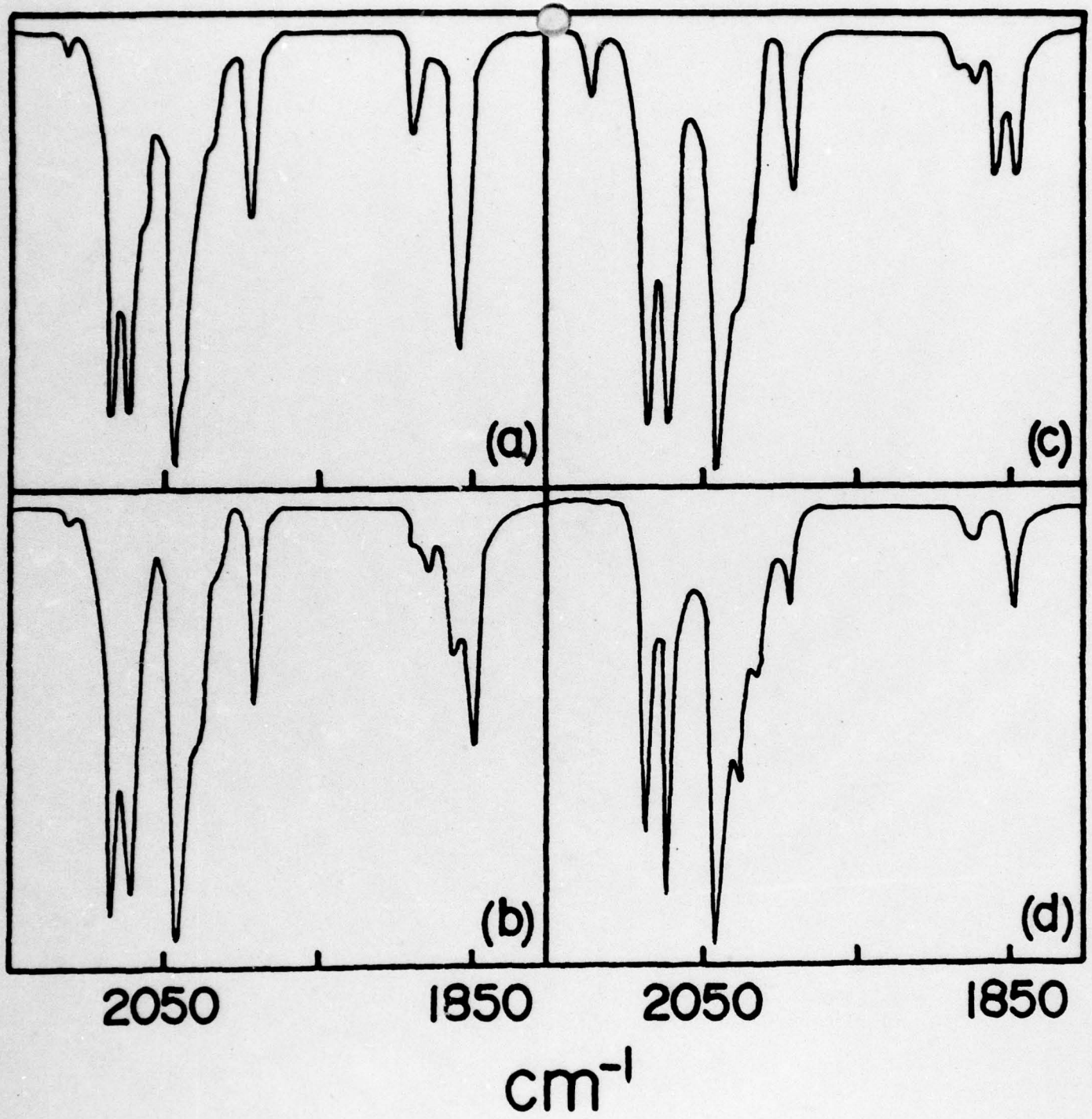
(a)
(c)
(b)
(d)
2050
1850
2050
1850
cm⁻¹

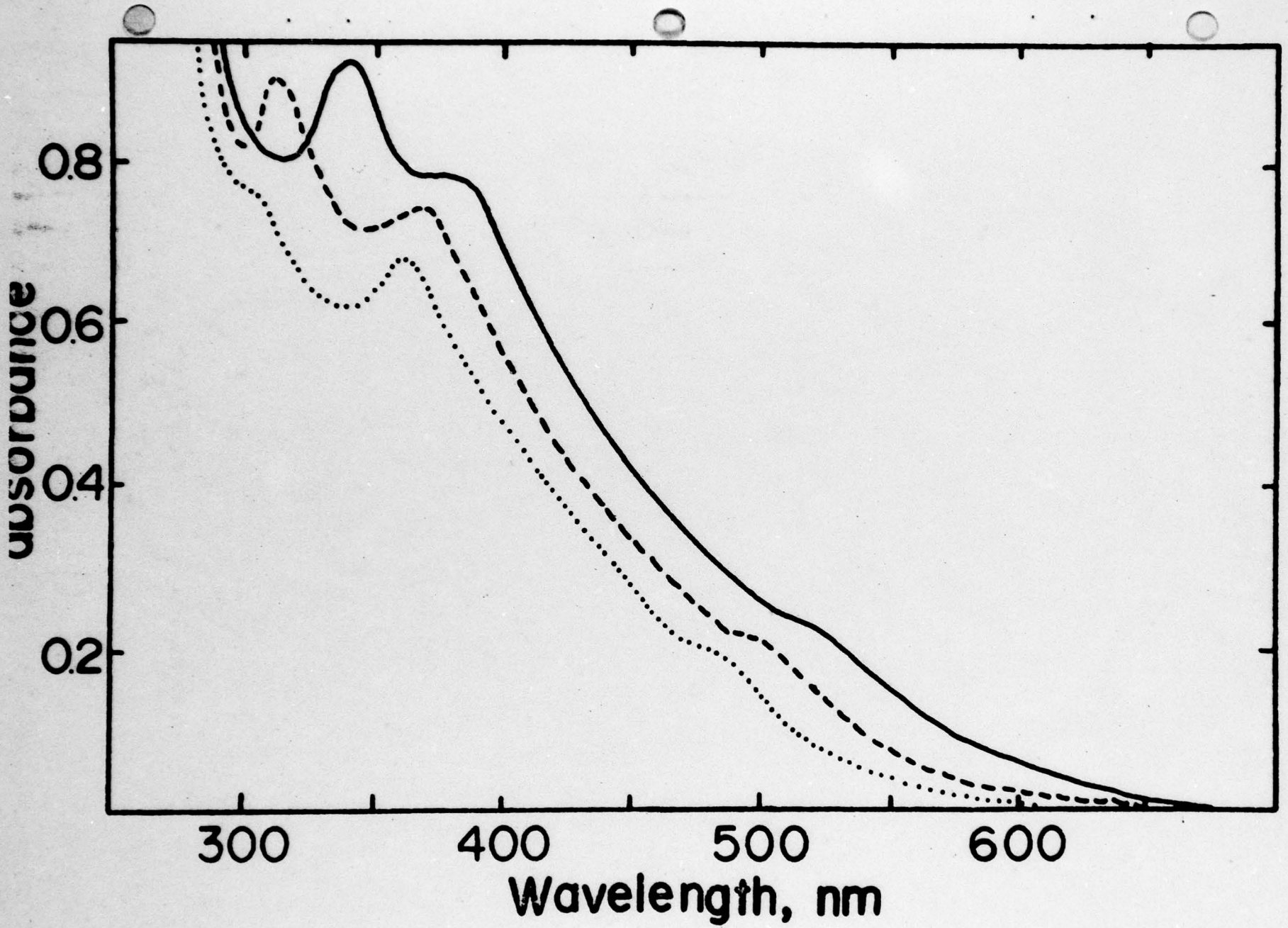
0.8
0.6
0.4
0.2
Absorbance
300
400
500
600
Wavelength, nm

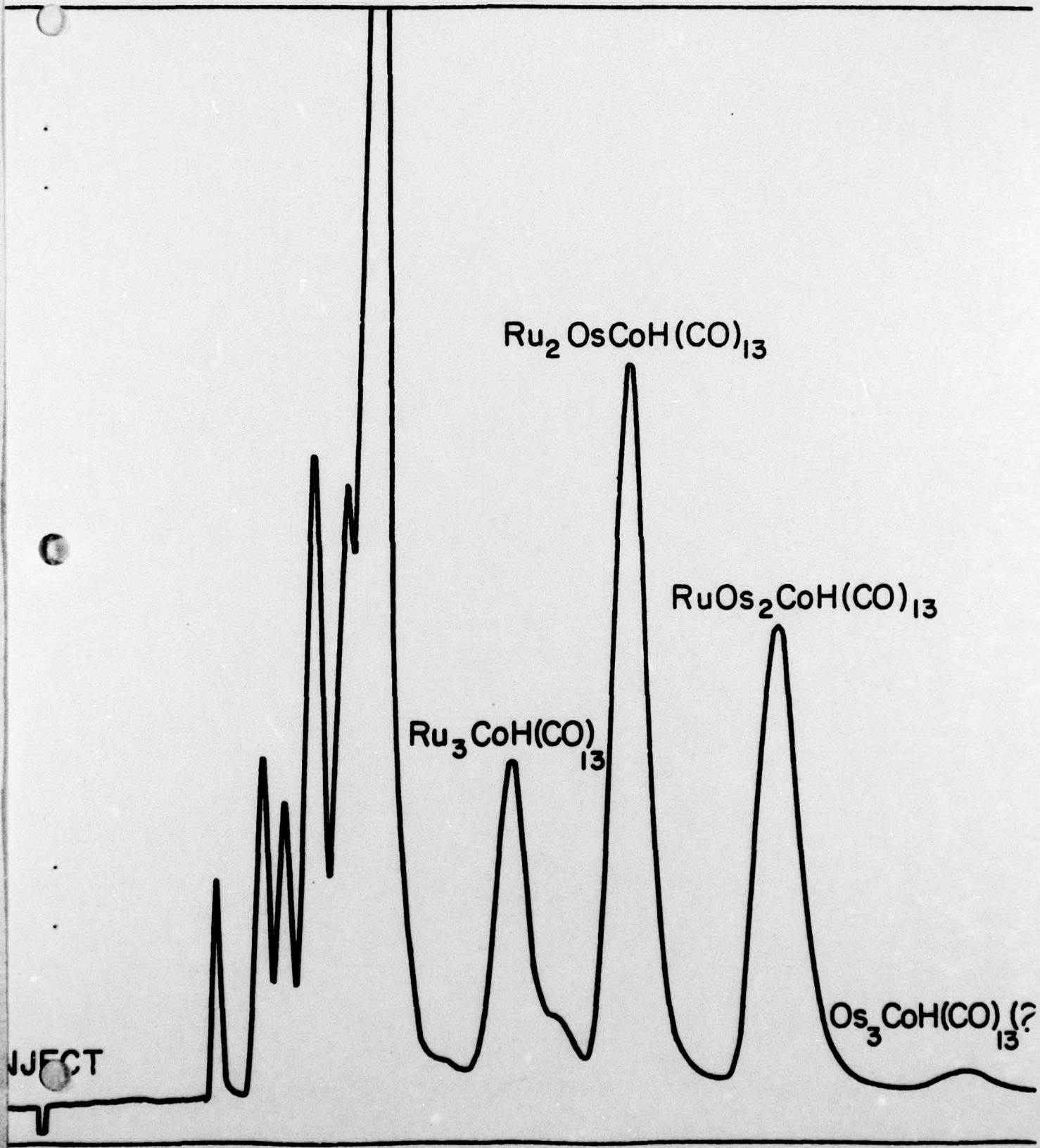
$Ru_2OsCoH(CO)_{13}$
$RuOs_2CoH(CO)_{13}$
$Ru_3CoH(CO)_{13}$
$Os_3CoH(CO)_{13}$ (?
NJECT

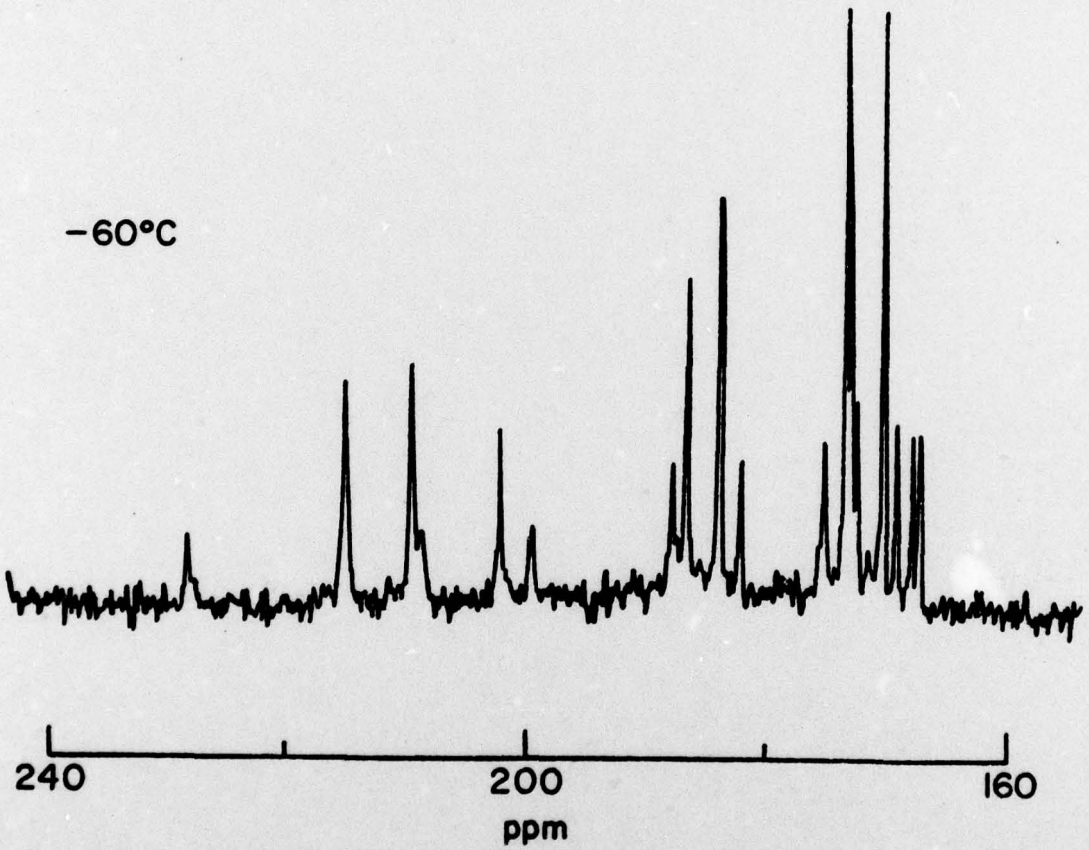
-60°C
240
200
160
ppm

TECHNICAL REPORT DISTRIBUTION LIST

	No. Copies
Office of Naval Research Arlington, Virginia 22217 Attn: Code 472	2
~~Office of Naval Research~~ ~~Arlington, Virginia 22217~~ ~~Attn: Code 102IP~~	~~1~~ ~~6~~
ONR Branch Office 536 S. Clark Street Chicago, Illinois 60605 Attn: Dr. Jerry Smith	1
ONR Branch Office 715 Broadway New York, New York 10003 Attn: Scientific Dept.	1
ONR Branch Office 1030 East Green Street Pasadena, California 91106 Attn: Dr. R. J. Marcus	1
ONR Branch Office 760 Market Street, Rm. 447 San Francisco, California 94102 Attn: Dr. P. A. Miller	1
ONR Branch Office 666 Summer Street Boston, Massachusetts 02210 Attn: Dr. L. H. Peebles	1
Director, Naval Research Laboratory Washington, D.C. 20390 Attn: Code 6100	1
The Asst. Secretary of the Navy (R&D) Department of the Navy Room 4E736, Pentagon Washington, D.C. 20350	1
Commander, Naval Air Systems Command Department of the Navy Washington, D.C. 20360 Attn: Code 310C (H. Rosenwasser)	1

	No. Copies
Defense Documentation Center Building 5, Cameron Station Alexandria, Virginia 22314	12
U.S. Army Research Office P.O. Box 12211 Research Triangle Park, N.C. 27709 Attn: CRD-AA-IP	1
Naval Ocean Systems Center San Diego, California 92152 Attn: Mr. Joe McCartney	1
Naval Weapons Center China Lake, California 93555 Attn: Head, Chemistry Division	1
Naval Civil Engineering Laboratory Port Hueneme, California 93041 Attn: Mr. W. S. Haynes	1
Professor O. Heinz Department of Physics & Chemistry Naval Postgraduate School Monterey, California 93940	1
Dr. A. L. Slafkosky Scientific Advisor Commandant of the Marine Corps (Code RD-1) Washington, D.C. 20380	1
Office of Naval Research Arlington, Virginia 22217 Attn: Dr. Richard S. Miller	1
ONR Resident Representative Room 407-MMCC Carnegie-Mellon University Pittsburgh, Pennsylvania	1

TECHNICAL REPORT DISTRIBUTION LIST

	No. Copies
Dr. R. M. Grimes University of Virginia Department of Chemistry Charlottesville, Virginia 22901	1
Dr. M. Tsutsui Texas A&M University Department of Chemistry College Station, Texas 77843	1
Dr. C. Quicksall Georgetown University Department of Chemistry 37th & O Streets Washington, D.C. 20007	1
Dr. M. F. Hawthorne University of California Department of Chemistry Los Angeles, California 90024	1
Dr. D. B. Brown University of Vermont Department of Chemistry Burlington, Vermont 05401	1
Dr. W. B. Fox Naval Research Laboratory Chemistry Division Code 6130 Washington, D.C. 20375	1
Dr. J. Adcock University of Tennessee Department of Chemistry Knoxville, Tennessee 37916	1
Dr. A. Cowley University of Texas Department of Chemistry Austin, Texas 78712	1
Dr. W. Hatfield University of North Carolina Department of Chemistry Chapel Hill, North Carolina 27514	1
Dr. D. Seyferth Massachusetts Institute of Technology Department of Chemistry Cambridge, Massachusetts 02139	1
Dr. M. H. Chisholm Princeton University Department of Chemistry Princeton, New Jersey 08540	1
Dr. B. Foxman Brandeis University Department of Chemistry Waltham, Massachusetts 02154	1
Dr. T. Marks Northwestern University Department of Chemistry Evanston, Illinois 60201	1
~~Dr. G. Geoffroy~~ ~~Pennsylvania State University~~ ~~Department of Chemistry~~ ~~University Park, Pennsylvania 16802~~	1
Dr. J. Zuckerman University of Oklahoma Department of Chemistry Norman, Oklahoma 73019	1